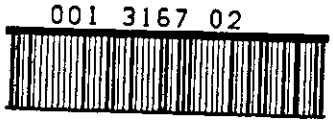

Synopsis: M.Phil Thesis by D. Belahrache

Studies of Air Cored Toroidal Inductors

The thesis is mainly concerned with some optimum designs for air cored toroidal inductors. It also describes theoretical and practical investigations of the inductance and losses of toroidal cage coils with the optimum Shafranov D shape.

Air cored toroidal inductors are used in many power electronics applications. Unlike solenoids they do not generate high external magnetic fields that can cause interference in other neighbouring components. They are also preferred to iron cored inductors because they do not have saturation problems.

The thesis has three main sections. The first outlines two different methods giving a family of optimum shapes for the cross section of an ideal thin toroidal inductor. A Fortran computer program was prepared for the numerical calculation of the optimum shape, its perimeter length, and the inductance of the whole toroid. The second part deals with the problem of winding the greatest possible inductance with a given length of wire for single layer toroids. It treats the problem of toroids with square, circular and D shape cross sections. In the case of D shape cross sections, the optimum radius-ratio has been determined. This means that the most economical design for single layer toroids,with both optimum turns and optimum shape, is obtained. In the third part, the toroidal cage coil, which is a special type of toroidal inductors that was invented to overcome practical manufacturing problems, exploits the Shafranov D shape for maximum field energy. Five cages have been prepared to test the accuracy of a theoretical inductance formula. Loss calculations and measurements are also given for alternating currents and the frequency-squared dependance of proximity effects is shown.

STUDIES OF AIR CORED TOROIDAL INDUCTORS

by

DJALAL BELAHRACHE

A Master's Thesis, submitted in
partial fulfilment of the requirements
for the award of Master of Philosophy
of the Loughborough University of Technology

January 1987

Supervisor: P. N. Murgatroyd, B.Sc., Ph.D., F.Ins.P., C.Eng.
Department of Electronic and Electrical Engineering

Dedication

To my family

ACKNOWLEDGEMENTS

My thanks are due to:

My supervisor, Dr. P. N. Murgatroyd, for his encouragement and constant guidance in all aspects of this work;

Mr. P. Barrington for the construction of the formers;

Mrs. N. Starosta for typing this thesis.

I also wish to thank the Algerian Ministry of Higher Education for their financial support.

CONTENTS

CHAPTER 1

INTRODUCTION

Inductors [1,2,3] are one of the essential elements which play important roles in electrical networks. They are passive components and have the property of opposing changes of currents flowing through them.

There is a wide variety of inductance coil types ranging from the large low frequency smoothing iron cored choke to the tiny high frequency tuning air cored inductor. Inductors may also be classified according to core material (air or iron), frequency (audio or radio), method of winding (solenoid, toroid, spiral, etc.), or application. Unlike resistors, capacitors and other components, inductors are generally made by the circuit designer. Nevertheless we can find miniature components with standardised values (100 nH to 100 mH) for use in telecommunication circuits [4].

The rapid progress in electronics with the advent of integrated circuits brought a big trend towards size reduction of circuitry, but the physical form of inductors as well as other magnetic components sometimes causes problems. Despite some successful attempts to replace or avoid inductive reactances, inductors remain essential circuit elements. For some applications there is no alternative but to concentrate on inductors themselves and find optimum designs.

One area of interest where inductors are considered as important circuit elements, and are still widely used, is the power electronics field. Here are a few examples of their uses [5]:

- To smooth the current in filters.
- To limit the rate of current rise in thyristors.
- To turn off thyristors in resonant commutation circuits.

Power electronics inductors, which are designed for low frequency applications, are generally large in physical dimensions because they are required to have large inductances and carry high currents. The inductance and the current rating are then the main factors which characterise an inductor. The first depends on the type of winding and core material, and the second defines the choice of the diameter of wire. Usually, the choice of an inductor is due to technical constraints. Iron cored inductors, for example, are avoided by some engineers because they have saturation problems. Some air-cored inductors, like solenoids, generate high magnetic fields that may interfere with other neighbouring components, for instance causing unwanted firings of thyristors.

One good solution, that has proved efficient in power electronics circuits, is the air-cored toroidal inductor which is becoming widely used. These coils have no saturation problems and confine their magnetic field very well. Indeed it is theoretically possible to wind a toroid with no external field whatever.

We can imagine the importance of toroidal windings when we know that the UK market required approximately £10m of toroidal coils and transformers in 1985 [6].

However, from an economic point of view, these inductors seem to have a worse position compared with simpler windings. They are more voluminous, and the manufacturing is not as easy as for solenoids. These disadvantages carry cost penalties.

Attempts are being made to reduce the labour content by automating the winding process. Optimisation studies are also being carried out to find the most economical designs and to find easier ways of winding toroids, like, for example, the toroidal cage coil [7].

CHAPTER 2

OPTIMUM DESIGNS FOR IDEAL THIN TOROIDS

2.1 Introduction

In 1960, Leites [8], who was working on high voltage power reactors for use in long distance transmission lines, studied the problem of winding toroidal reactors with no bending stresses. His calculations led him to a second order differential equation from which he plotted the curve of the cross-section shape of the toroid using a step by step graphical method.

Working in the context of research on thermonuclear reactors like the tokamak type, File et al [9], in 1971, used the same method and obtained the expression of the first derivative of the curve which they integrated numerically. After their work, the shape is sometimes referred to as the "Princeton-D", but it is better known as the "D-shape" because it resembles the letter D.

A year later, Shafranov [10] examined the problem of finding the optimum shape of an ideal toroidal coil to ensure maximum field energy for a fixed length of coil material. He arrived at the same result as File et al, which consisted of a family of shapes depending on the ratio of inner to outer radii of the toroid.

The two methods are reviewed in the next two sections.

Ten years after Shafranov, Murgatroyd [11] showed that their result, and particularly as stated by Shafranov, could be used in the practical design of inductors. He did a further study including optimum shapes for alternating currents.

2.2 Magnetic Field Energy Method

A toroidal coil is a long solenoid bent into a circular shape. In an ideal thin toroidal coil the windings are thin in comparison with the overall dimensions, and the turns are very close. Application of Ampere's theorem to circular paths shows that all the magnetic field is confined within the coil (not completely true for practical coils). At a radius r from the mean axis of the toroid, it is given by

$$B = \frac{\mu_o NI}{2\pi r} \qquad (2.2.1)$$

The stored magnetic field energy is given by

$$\frac{1}{2} LI^2 = \int \frac{B^2 dV}{2\mu_o} \qquad (2.2.2)$$

It is evident that an optimum toroid must have an equatorial plane of symmetry because one half cannot perform

better than the other. A general formula can be derived for the inductance of a toroidal coil with an arbitrary cross-section, but with a plane of symmetry that coincides with the surface z = o, as dimensioned in Fig. 2.1.

Combining equations (2.2.1) and (2.2.2) yields

$$L = \frac{\mu_o N^2}{\pi} \int_b^c \frac{z(r)}{r}\, dr \qquad (2.2.3)$$

From a similar equation and the expression of the perimeter of the cross-section, Shafranov recognized an isoperimetric problem of the calculus of variations [12]. Following his theory, the curve z(r), which defines the optimum shape, has vertical tangents at both ends.

Although they did not affect the final result, Murgatroyd noticed that any lengths of finite straight portions that the shape may possibly have at the inner and outer radii had not been included by Shafranov, and so added them in the calculations.

The perimeter of the cross-section is thus given by

$$l = 2 \int_b^c \sqrt{1 + s^2}\, dr + 2\,(z(b) + z(c)) \qquad (2.2.4)$$

where $s = \frac{dz}{dr}$ is the slope of the curve at a point (r, z)

Equation (2.2.4) can be converted to the pure integral

$$1 = 2\int_b^c \left[\sqrt{1+s^2} + \frac{2}{c-b}\left(rs + z - \left(\frac{b+c}{2}\right)s\right)\right] dr \qquad (2.2.5)$$

The problem is then the determination of the function $z = z(r)$ for which the integral

$$G[z] = \int_b^c \frac{z(r)}{r}\, dr \qquad (2.2.6)$$

takes the largest value subject to the conditions

$$K[z] = \int_b^c \left[\sqrt{1+s^2} + \frac{2}{c-b}\left(rs+z - \frac{b+c}{2}\, s\right)\right] dr \qquad (2.2.7)$$

and

$$\frac{dz}{dr} = \infty \qquad \text{at } r = b \text{ and } r = c \qquad (2.2.8)$$

To deal with this isoperimetric problem, we form the functional

$$G[z] + \lambda K[z] = \int F(r)\, dr \qquad (2.2.9)$$

with

$$F(r) = \frac{z}{r} + \lambda\left[\sqrt{1+s^2} + \frac{2}{c-b}\left(rs+z - \frac{b+c}{2}\, s\right)\right] \qquad (2.2.10)$$

and write the corresponding Euler-Lagrange equation

$$\frac{\partial F}{\partial z} - \frac{d}{dr}\frac{\partial F}{\partial s} = \frac{1}{r} + \lambda \frac{d}{dr}\frac{s}{\sqrt{1+s^2}} = 0 \qquad (2.2.11)$$

which implies

$$\frac{dr}{r} = \lambda d\left(\frac{s}{\sqrt{1+s^2}}\right) \qquad (2.2.12)$$

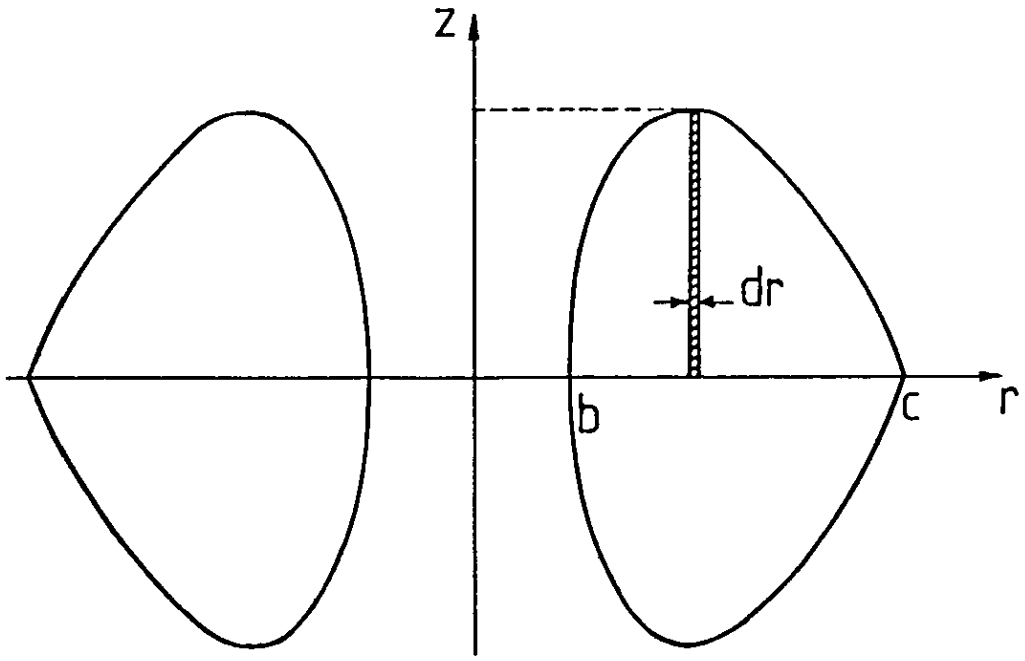

Fig. 2.1 Ideal thin toroid with arbitrary but symmetrical cross section.

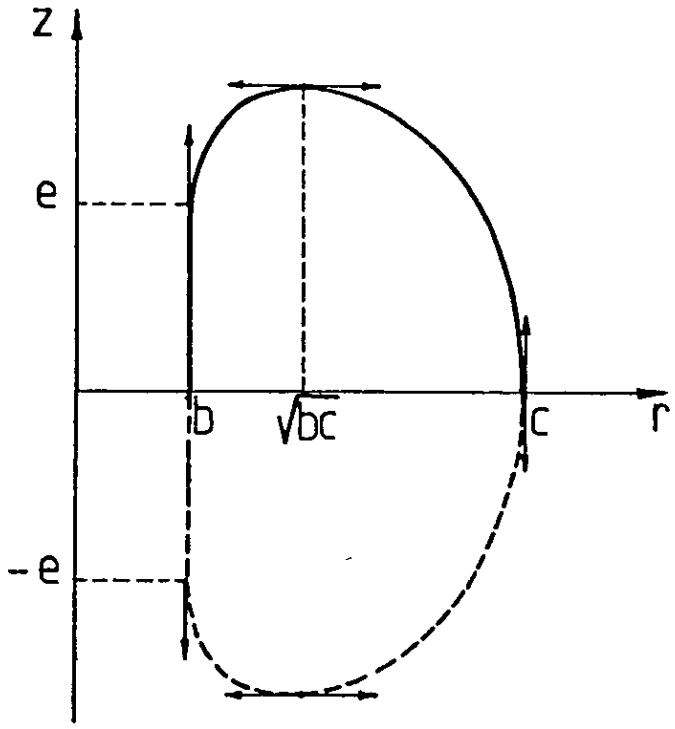

Fig. 2.2 Appearance of the optimum cross-section shape of an ideal thin toroid.

Integrating (2.2.12) we obtain the equation

$$\frac{dz}{dr} = \pm \frac{Ln(r/k)}{\sqrt{\lambda^2 - Ln^2(r/k)}} \qquad (2.2.13)$$

The values of k and λ are constants which are determined from the conditions given by equation (2.2.6)

at r = b we have $\lambda^2 - Ln^2(b/k) = o$ (2.2.14)

and at r = c we have $\lambda^2 - Ln^2(c/k) = o$ (2.2.15)

The solution of the system composed by equations (2.2.14) and (2.2.15) yields

$$\lambda = \frac{1}{2} Ln(b/c) \qquad (2.2.16)$$

and $$k = \sqrt{bc} \qquad (2.2.17)$$

The curve z(r) and its symmetrical are then given by the expression

$$\frac{dz}{dr} = \pm \frac{Ln(\sqrt{bc}/r)}{\sqrt{Ln(r/b)Ln(c/r)}} \qquad (2.2.18)$$

We can easily notice that the curve has a maximum for $r = \sqrt{bc}$. The solution of equation (2.2.18) is explained in the last section of this chapter, but a first sketch of the appearance of the curve z(r) is given in Fig. 2.2.

2.3 Mechanical Strength Method

Large toroidal windings are frequently used in thermonuclear fusion technology because they produce fields in which the magnetic lines of forces close up on themselves and provide good confinement for the plasma within the working volume [13]. They are also used as current limiting devices in high power transmission systems [8].

In this type of reactor, the high current in the windings together with the magnetic field it creates produce forces which tend to expand the coil. Because the forces are not uniformly distributed, this kind of internal magnetic pressure subjects the reactor to some bending stresses and hence deformations. In fact the system tends to have a state of equilibrium. It is possible to keep the windings in position by using very strong structures, but this method is very costly.

A better solution is to minimise the bending stresses by choosing a toroid where the windings are in pure tension. In other words, the cross-section of the toroid should have a shape in such a way that the tension is the same all the way round.

Along an arc dl, the force F (see Fig. 2.3) is related to the radius of curvature R and the tension T, which has to be constant, by the expression [14]

$$T = R \frac{F}{dl} = \text{cste} \qquad (2.3.1)$$

Since the force is like IdlB and B is proportional to $\frac{1}{r}$, equation (2.3.1) becomes

$$pR = r \qquad (2.3.2)$$

where p is a constant.

The radius of curvature is given by [15]

$$R = \pm \frac{(1 + u^2)^{3/2}}{du/dr} \qquad (2.3.3)$$

where $u = \frac{dr}{dz}$ is the inverse of the slope at a point (r,z)

Combining equations (2.3.2) and (2.3.3) yields

$$p \frac{dr}{r} = \pm \frac{udu}{(1+u^2)^{3/2}} \qquad (2.3.4)$$

This equation can be integrated once to give

$$pLn(r/q) = \pm 1/(1+u^2)^{1/2} \qquad (2.3.5)$$

where q is a constant

whence

$$\frac{1}{u} = \frac{dz}{dr} = \pm \frac{Ln(r/q)}{\sqrt{p^2-Ln^2(r/q)}} \qquad (2.3.6)$$

This equation is exactly the same as equation (2.2.13). It is not a coincidence, but it is simply due to the fact that stable equilibrium corresponds to minimum free energy [16].

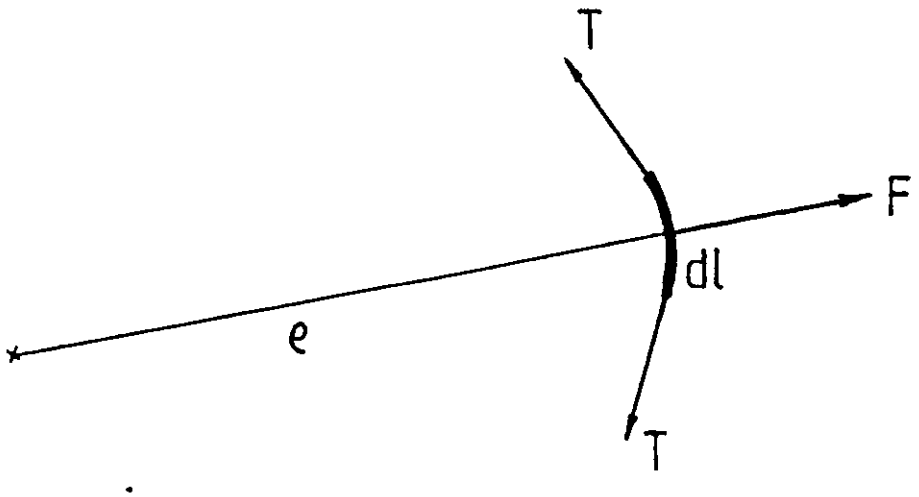

Fig. 2.3 Forces acting on an element dl in a toroidal reactor.

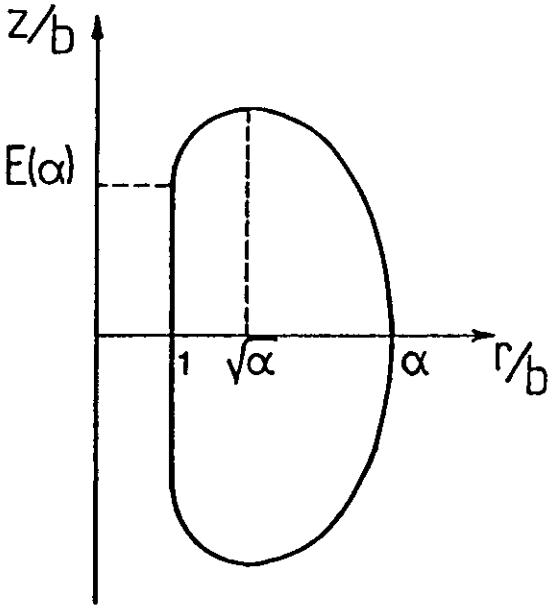

Fig. 2.4 Optimum cross-section shape with dimensionless quantities

2.4 Numerical Solution

As mentioned before, the solution for the shape of an idealised constant tension coil was done by Leites via a graphical technique, whereas File et al, Shafranov, and Murgatroyd performed it using numerical methods. The analytical solution was given in 1976 by Gralnick and Tenney [17] in terms of modified Bessel functions of the first kind.

In his method, Murgatroyd used the Runge Kutta method [18] and implemented it in an Algol program. At the ends of the curve, where the slope is infinite and where the Runge Kutta method cannot be applied, he employed analytical approximations to equation [2.2.18].

In the present work, the fourth order Runge Kutta method and the third order Taylor's expansion, for the ends of the range where the slope is infinite, are implemented in a Fortran 77 program on the Multics computer of Loughborough University.

The program with details is given in Appendix 1.

The trapezoidal method is also implemented in the same program to evaluate the inductance and the perimeter of the cross-section.

For convenience and to have a more general result, the numerical integration is performed in dimensionless quan-

tities depending on the radius ratio $\alpha = c/b$ (see Fig. 2.4). All quantities are then expressed in terms of the inner radius b and a function of α.

$$L = \frac{\mu_o N^2}{2} b\, S(\alpha) \qquad (2.4.1)$$

$$l = bP(\alpha) \qquad (2.4.2)$$

$$e = bE(\alpha) \qquad (2.4.3)$$

where $S(\alpha)$, $P(\alpha)$ and $E(\alpha)$ are successively the computed dimensionless inductance, the dimensionless perimeter of the cross-section and the length of the straight portion at $\alpha = 1$.

A family of computed D-shape cross-sections is given in Fig. 2.5.

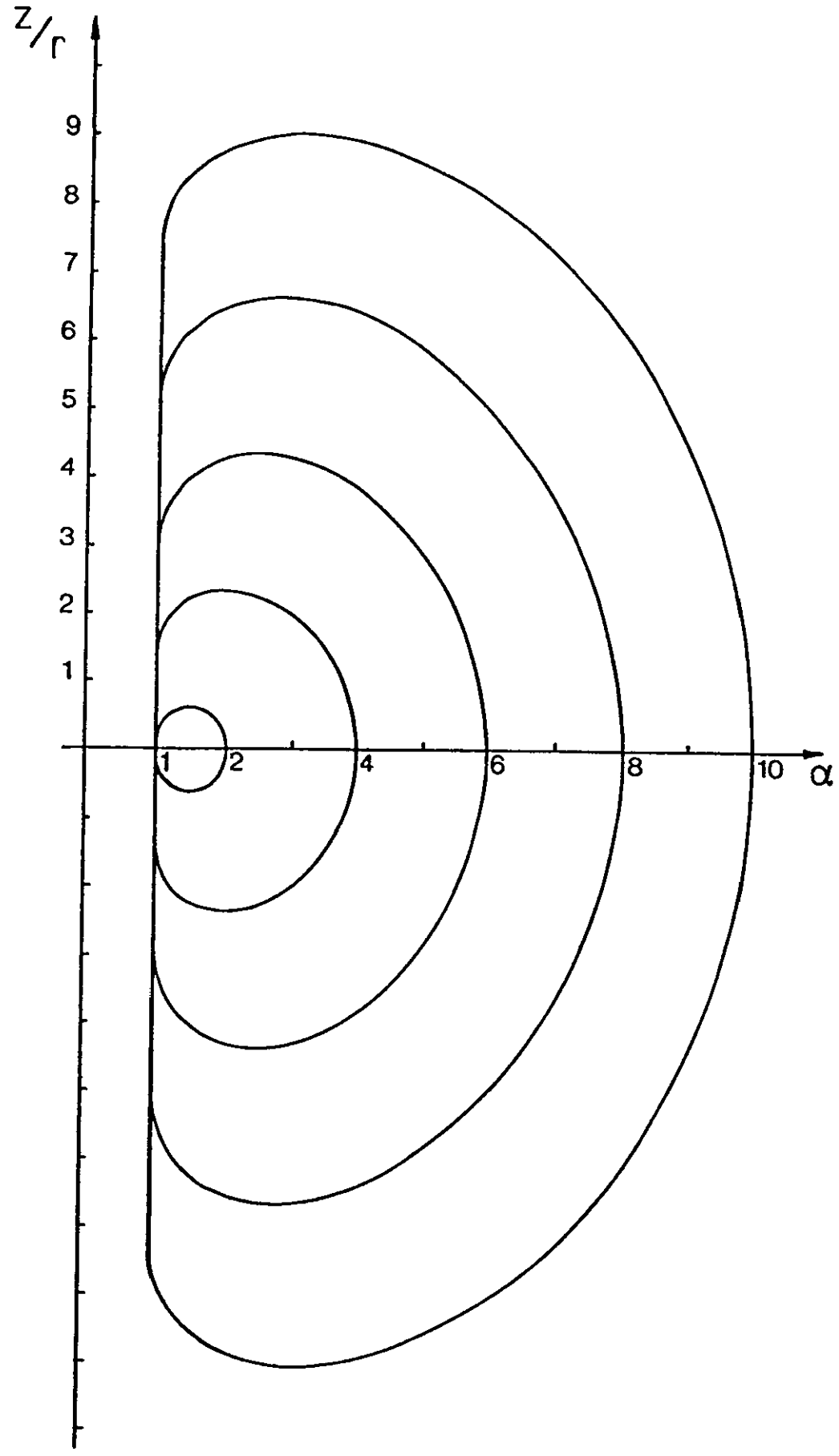

Fig. 2.5 A family of computed optimum toroid cross-sections.

CHAPTER 3

OPTIMUM DESIGNS FOR SINGLE LAYER TOROIDS

3.1 Introduction

There are many different ways of winding an inductor of a given type to obtain a certain inductance value. Practical engineers prefer one design to another for technical or economic reasons. From the economic point of view, the best design is one in which a minimum of coil material is used.

In the last century, Maxwell [19] examined the problem of the best way of winding a given length of wire into a solenoid to achieve the greatest inductance possible. His solution was a square cross-section solenoid in which the mean turn diameter was 3.7 times the side of the square. Shawcross and Wells [20] used a better formula than Maxwell and showed that the ratio should be 3. Finally, Brooks [21] whose name is associated with the optimum design, showed that the mean diameter is in fact 2.967 times the side of the square.

The present chapter describes the first investigation of a similar problem concerning single layer toroidal inductors. Fig. 3.1 shows two different possibilities of winding a single layer toroid with a fixed length of wire of a given diameter. An infinite number of other ways is possible,

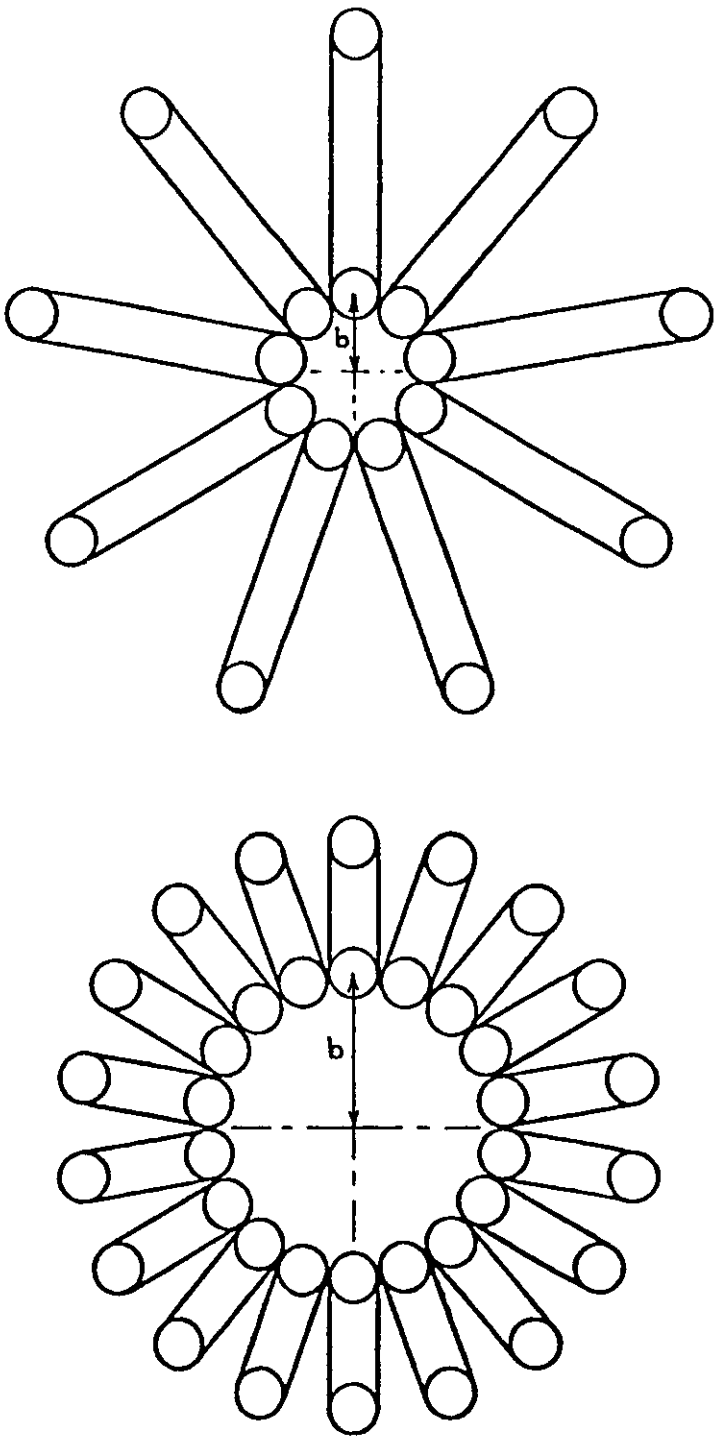

Fig. 3.1 Two different possibilities of winding single-layer toroidal inductors using the same wire-length.

but it is obvious that any constructions in which the wires are not in close contact at the inner radius must be less efficient than constructions where the centre of the coil is more compact. It is also noticeable that a gain of inductance due to an increase of the number of turns will be reduced by a decrease of the turn area, and vice versa. Therefore there has to be a compromise, and the following calculations show that the maximum inductance is achievable if the number of turns is correctly chosen.

Optimum designs for toroids with square, circular, and D-shape cross-sections are analysed and compared.

3.2 Toroids with Square Cross-sections

The general inductance formula of a single layer toroidal inductor is given by

$$L = \frac{\mu_o N^2}{\pi} \int_b^c \frac{z(r)}{r}\, dr + \frac{\mu_o w}{8\pi} \qquad (3.2.1)$$

Here, the first term corresponds to the inductance of a thin toroid, which is given by equation (2.2.3), and the second term corresponds to the internal inductance of the of the wire of length w.

The turns of the toroid touch around the circumference of a circle of radius b (see Fig. 3.1). This geometrical arrangement allows us to write a wire contact condition

between the inner radius b, the wire diameter d, and the number of turns N (see Fig. 3.2) for any given cross-section; that is

$$b = \frac{d}{2 \sin (\pi/N)} \qquad (3.2.2)$$

The inductance of a square section toroid, as dimensioned in Fig. 3.3, may be obtained from equation (3.2.1) in which z(r) is constant at $\frac{1}{2}(c-b)$

$$L_s = \frac{\mu_o N^2}{2\pi} (c - b) \text{ Ln } (\frac{c}{b}) \qquad (3.2.3)$$

The side of the square is given by

$$c - b = \frac{w}{4N} \qquad (3.2.4)$$

Introducing the wire contact condition and equation (3.2.4) into equation (3.2.3), the inductance formula becomes

$$L_s = \frac{\mu_o N w}{\pi} \text{ Ln } \left[1 + \frac{w}{2Nd} \sin (\pi/N) \right] + \frac{\mu_o w}{8\pi} \qquad (3.2.5)$$

For convenience, the inductance may be expressed in terms of the scale inductance

$$L_o = \frac{\mu_o d}{2\pi} \qquad (3.2.6)$$

and the dimensionless wire-length

$$k = \frac{w}{d} \qquad (3.2.7)$$

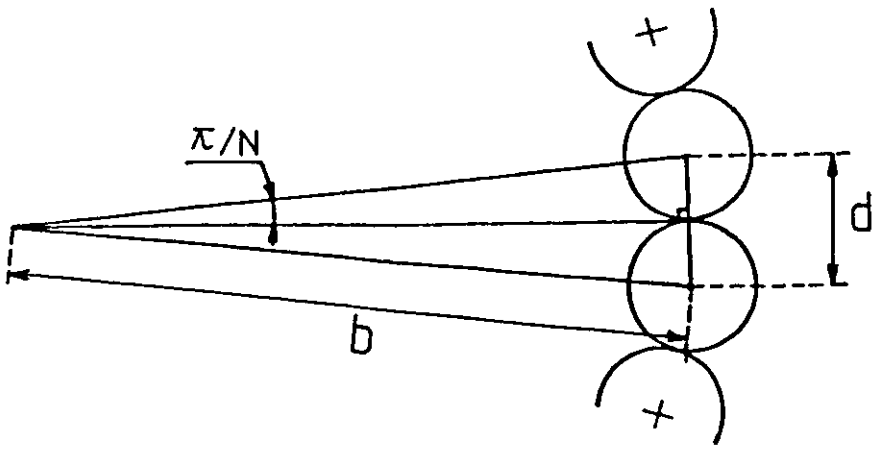

Fig. 3.2 Geometry of the wire contact at the inner radius.

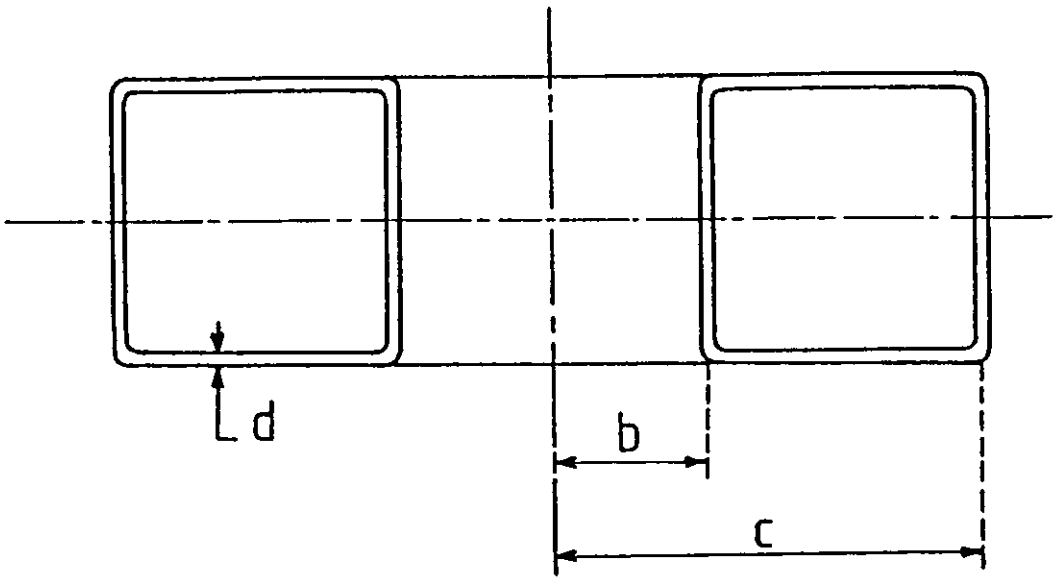

Fig. 3.3 Single-layer toroidal winding with square cross-section.

With these substitutions

$$\frac{L_s}{L_o} = \frac{Nk}{4} \text{Ln} \left[1 + \frac{k}{2N} \sin (\pi/N) \right] + \frac{k}{4} \qquad (3.2.8)$$

The dimensionless inductance L_s/L_o is plotted against the number of turns N for a range of values of the dimensionless wire-length k (see Fig. 3.4). Every curve is seen to have a soft optimum. The optimum values of N, which are integers, may easily be determined by tabulation. Plots of the optimum numbers of turns and the maximum dimensionless inductances against k on a logarithmic scale show linear dependences (see Fig. 3.5 and Fig. 3.6).

A direct differentiation of the function in equation (3.2.5) does not lead to an analytical solution. So the approximation $\sin (\pi/N) \simeq \pi/N$ for N large is used, and yields

$$\frac{L_s}{L_o} \longrightarrow \frac{Nk}{4} \text{Ln} \left(1 + \frac{\pi k}{2N^2} \right) + \frac{k}{4} \qquad (3.2.9)$$

To find the value of N that maximises this function, we make its derivative zero; that is

$$\text{Ln}(2x) - 4x + 2 = 0$$

or

$$x - \frac{1}{4} \text{Ln} (2x) - \frac{1}{2} = 0 \qquad (3.2.10)$$

where

$$\frac{1}{2x} = 1 + \frac{k}{2N^2} \qquad (3.2.11)$$

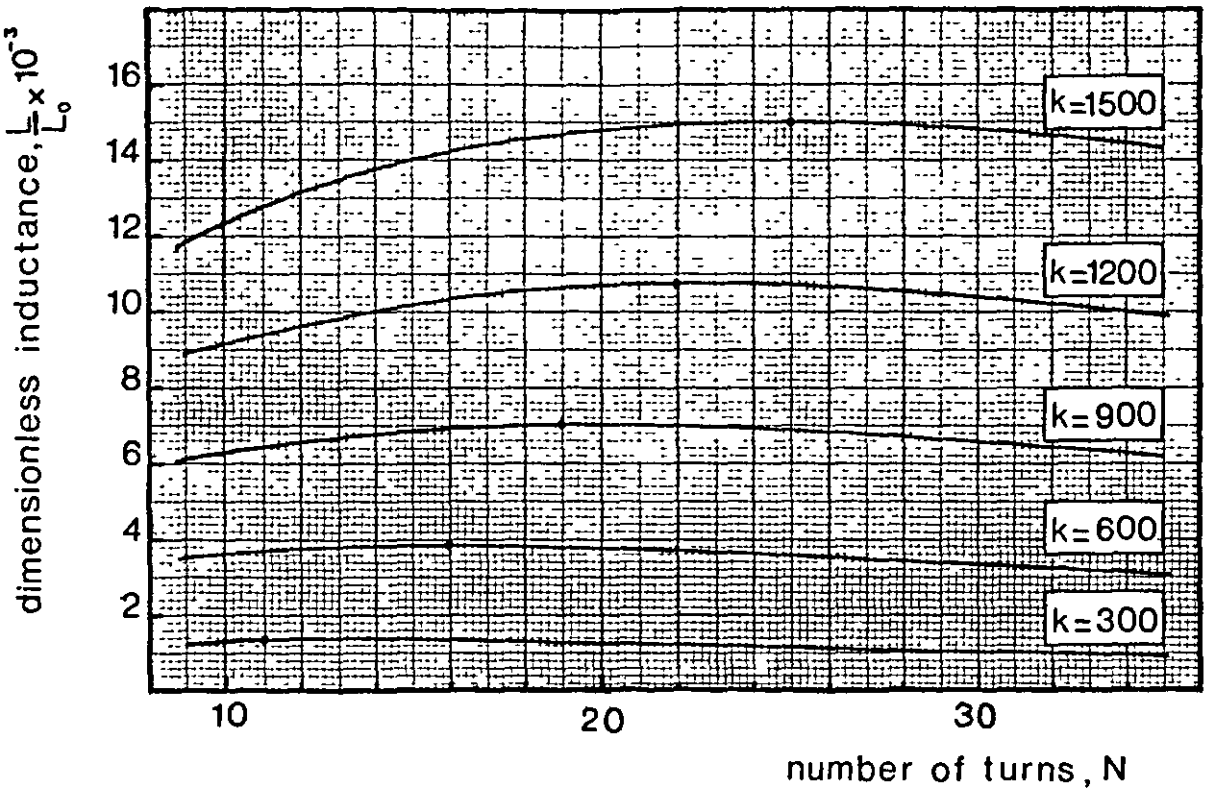

Fig. 3.4 Dimensionless inductance of a square-section toroid as a function of the number of turns for fixed wire-lengths.

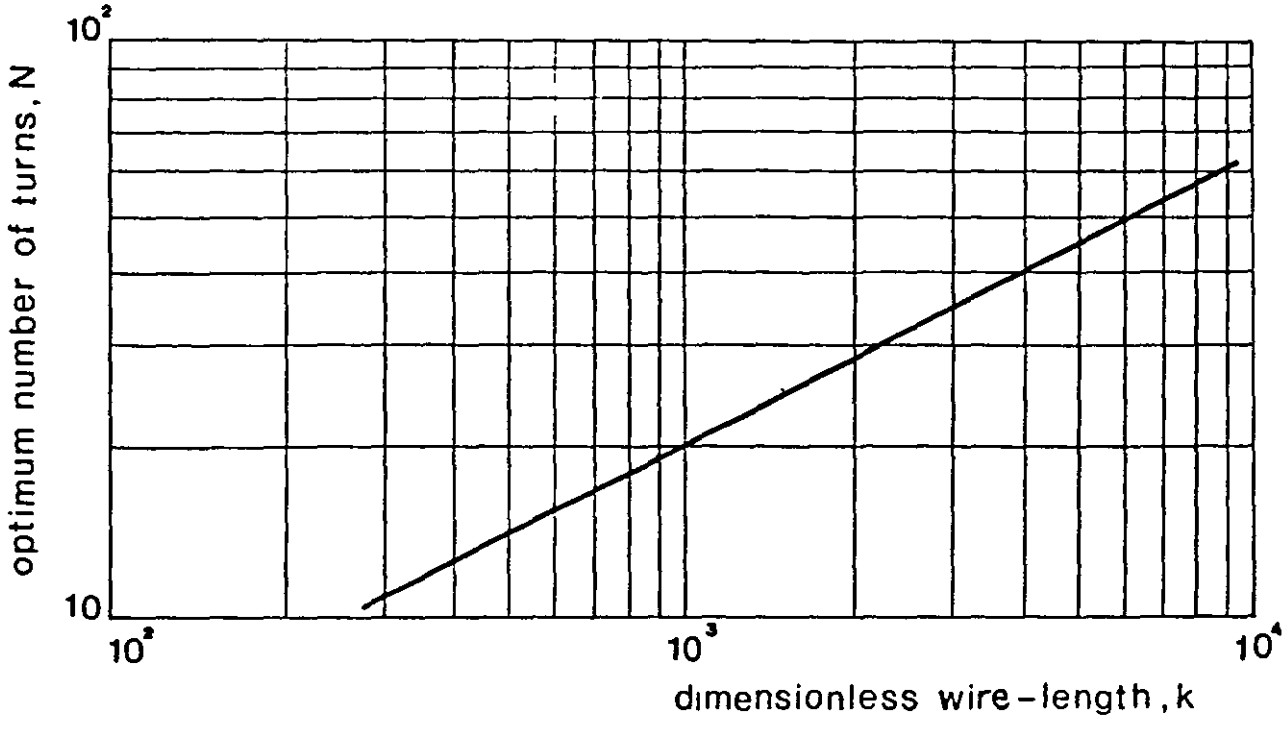

Fig. 3.5 Dependance of optimum number of square turns on wire-length.

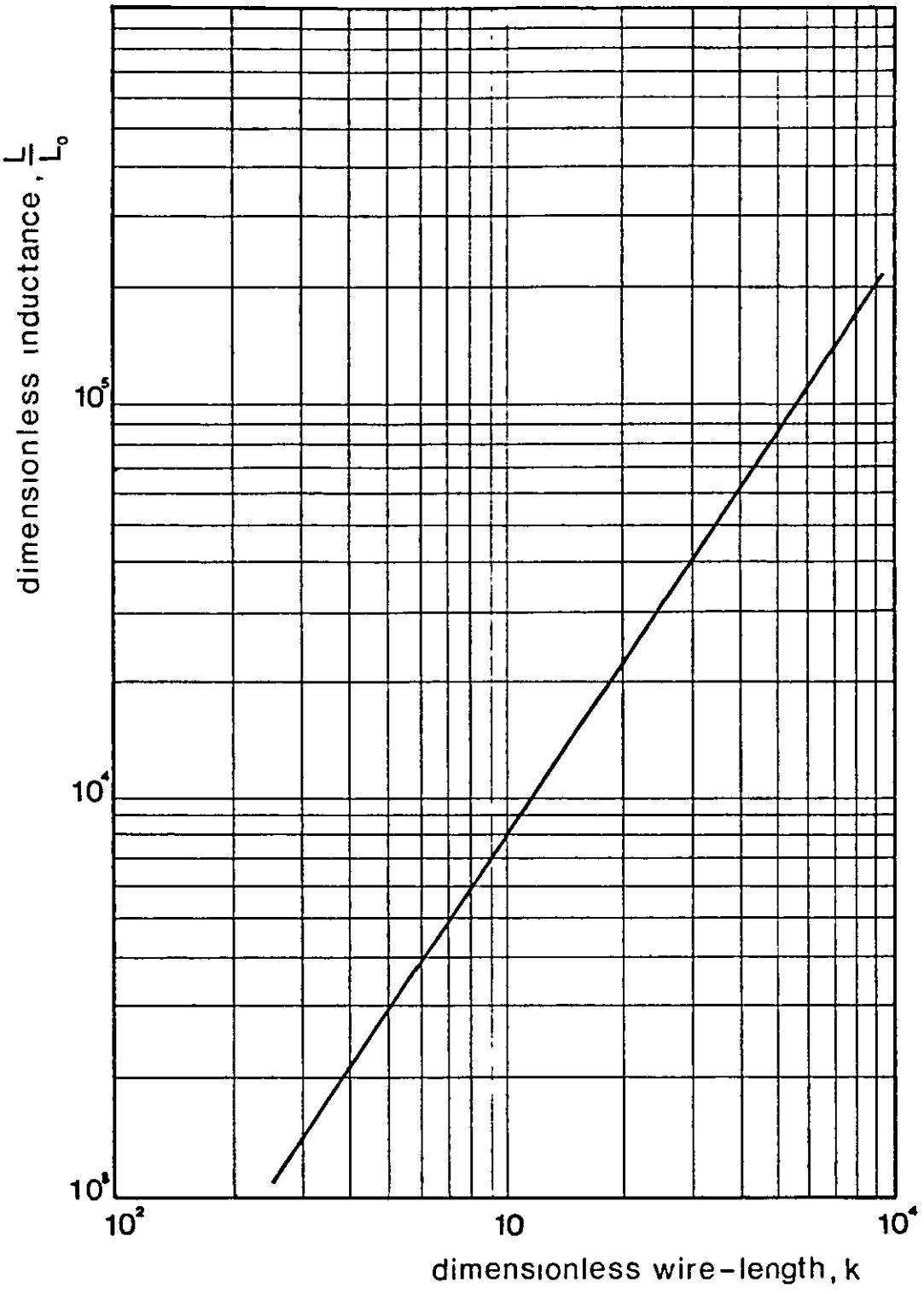

Fig. 3.6 Dependance of maximum square-section toroid inductance on wire-length.

The solution of equation (3.2.10) is achieved using the iterative method. It is given in Appendix 2, and the wanted value is

$$x = 0.1016 \qquad (3.2.12)$$

Substituting x by its value in equation (3.2.11) yields

$$N = 0.6329 \sqrt{k} \qquad (3.2.13)$$

When this is put back into equation (3.2.9), the best inductance is given by

$$\frac{L_s}{L_o} = 0.2522\ k^{3/2} + 0.25\ k \qquad (3.2.14)$$

3.3 Toroids with Circular Cross-sections

The inductance of a circular section toroid may be derived from equation (3.2.1) or found in many textbooks [1,3]. As dimensioned in Fig. 3.7, where z(r) has the expression of a semi-circle of diameter (c-b), it is given by

$$L_c = \mu_o N^2 \left[\frac{b + c}{2} - \sqrt{bc} \right] \qquad (3.3.1)$$

The diameter of the circle is given by

$$c - b = \frac{w}{\pi N} \qquad (3.3.2)$$

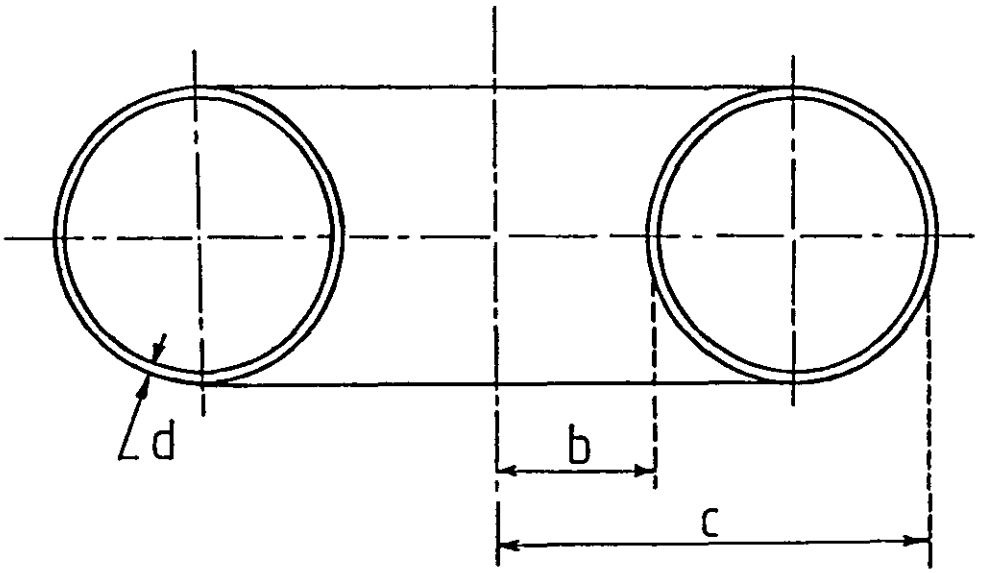

Fig. 3.7 Single-layer toroidal winding with circular cross-section.

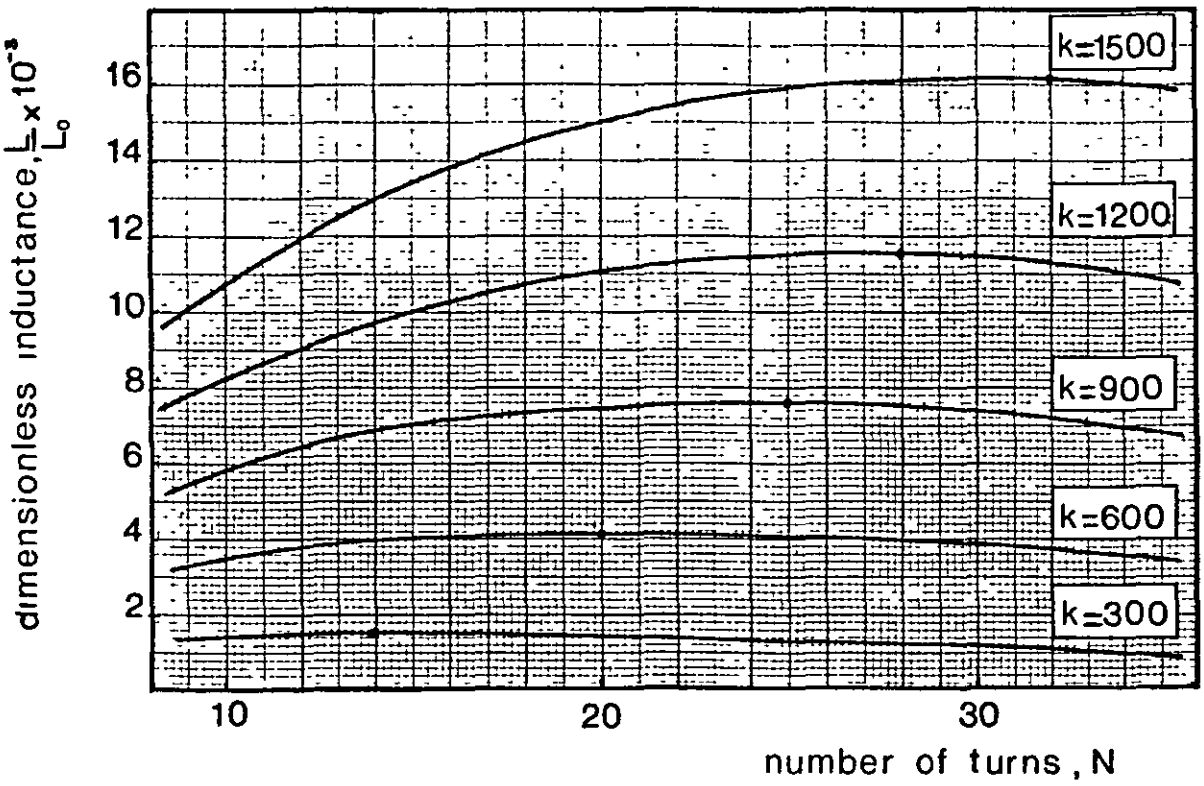

Fig. 3.8 Dimensionless inductance of a circular-section toroid as a function of the number of turns for fixed wire-lengths.

Introducing this expression and the wire contact condition given by equation (3.2.2) into equation (3.3.1), the inductance becomes

$$L_c = \mu_o N^2 \left[\frac{w}{2\pi N} + \frac{d}{2 \sin(\pi/N)} - \sqrt{\frac{d}{2 \sin(\pi/N)} \left(\frac{d}{2 \sin(\pi/N)} + \frac{w}{\pi N} \right)} \right] + \frac{\mu_o w}{8\pi} \qquad (3.3.3)$$

This formula may be rewritten in terms of the scale inductance and the dimensionless wire length introduced previously

$$\frac{L_c}{L_o} = N^2 \left[\frac{k}{N} + \frac{}{\sin(\pi/N)} - \sqrt{\frac{\pi^2}{\sin^2(\pi/N)} + \frac{2k\pi}{N \sin(\pi/N)}} \right] + \frac{k}{4} \qquad (3.3.4)$$

The dimensionless inductance L_c/L_o is plotted against the number of turns N, for a range of values of k (see Fig. 3.8). Here, also, every curve is seen to have a soft optimum. Similarly to the square section toroid, plots of the maximum dimensionless inductances and the optimum numbers of turns against k, on a logarithmic scale, show linear dependences (see Fig. 3.9 and Fig. 3.10).

For N large, $\sin(\pi/N)$ is approximated by (π/N) in equation (3.3.4)

$$\frac{L_c}{L_o} \longrightarrow N^2 \left[N + \frac{k}{N} - \sqrt{N^2 + 2k} \right] + \frac{k}{4} \qquad (3.3.5)$$

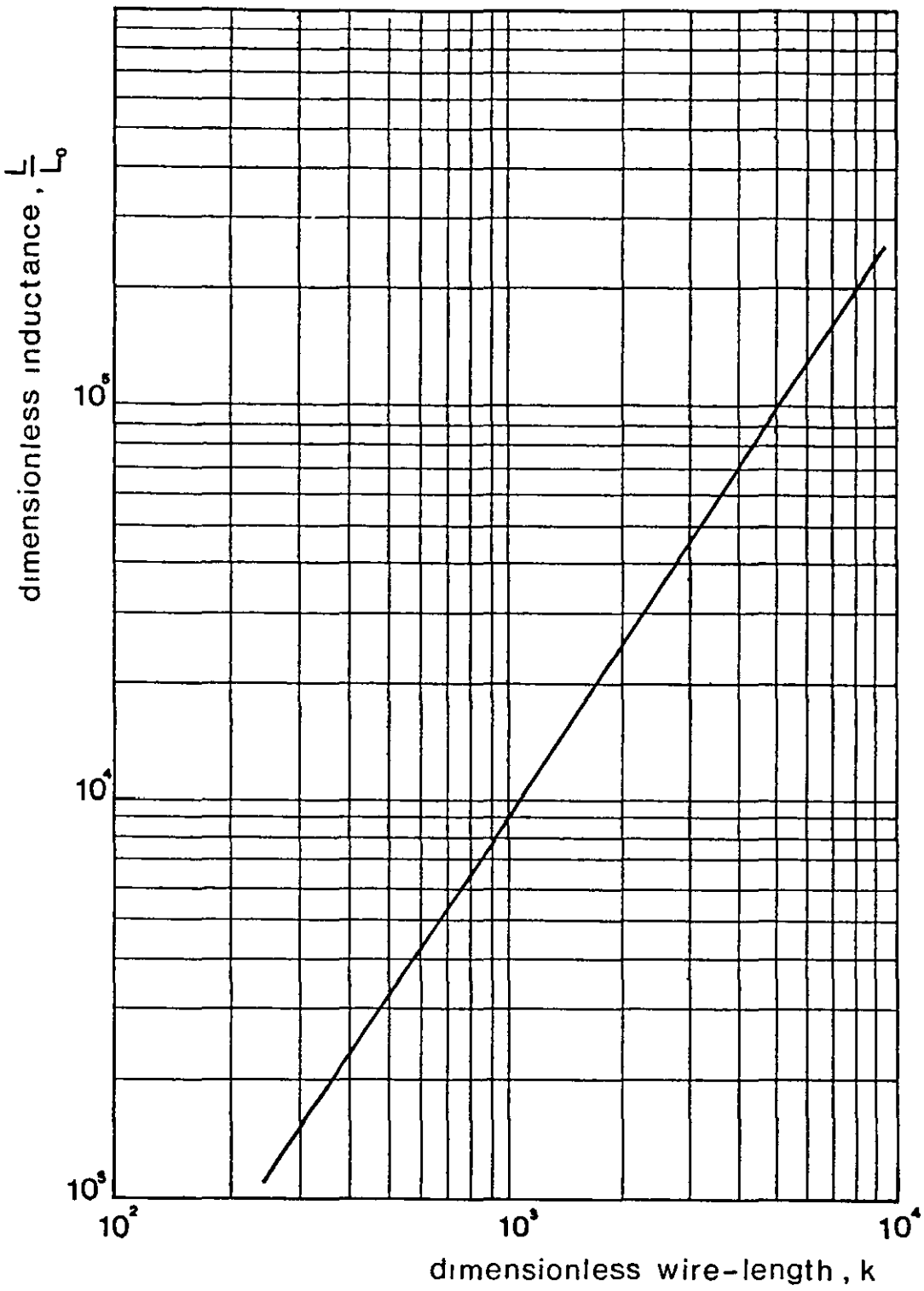

Fig. 3.9 Dependance of maximum circular-section toroid inductance on wire-length.

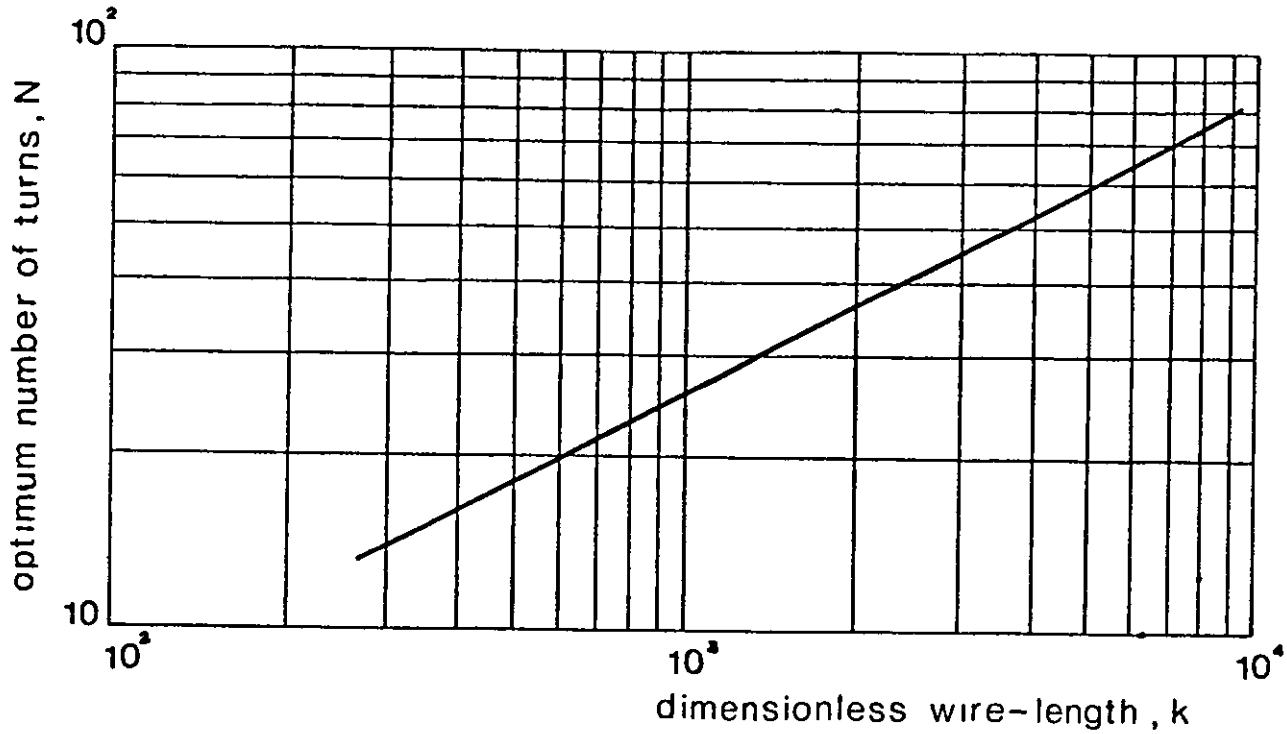

Fig. 3.10 Dependance of optimum number of circular turns on wire-length.

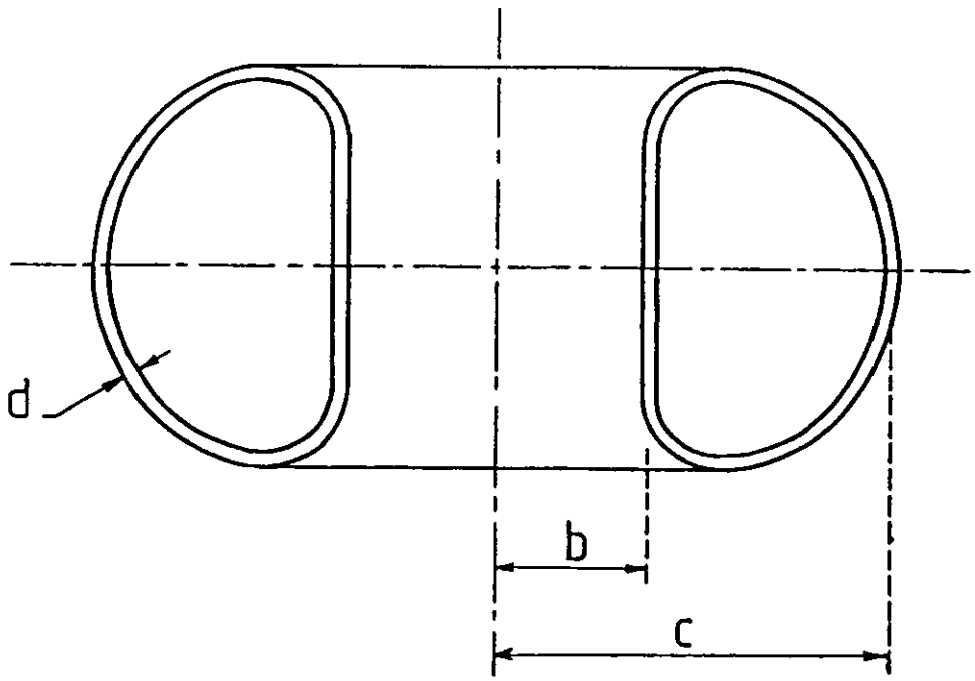

Fig. 3.11 Single-layer toroidal winding with D-shape cross-section.

To find the optimum number of turns, we make the derivative zero

$$N^2 - \frac{2}{3} k = o \qquad (3.3.6)$$

which implies

$$N = \sqrt{\frac{2}{3}} \sqrt{k}$$

or $$N = 0.8165\ k^{1/2} \qquad (3.3.7)$$

When this is put back into equation (3.3.5), the best inductance is given by

$$\frac{L_c}{L_o} = 0.2722\ k^{3/2} + 0.25\ k$$

3.4 Toroids with D-shape Cross-sections

The inductance of a D-shape cross-section single layer toroid, as dimensioned in Fig. 3.11, is given by

$$L_D = \frac{\mu_o}{2\pi} N^2\ b\ S(\alpha) + \frac{\mu_o w}{8\pi} \qquad (3.4.1)$$

where the first term corresponds to the inductance of a thin toroid, which is given by equation (2.4.1), and the second term is the internal inductance of the wire.

The inner radius is given from equation (2.4.2) by

$$b = \frac{1}{P(\alpha)} = \frac{w}{NP(\alpha)} \qquad (3.4.2)$$

Introducing this expression into equation (3.4.1), the inductance formula becomes

$$L_D = \frac{\mu_o}{2\pi} Nw \frac{S(\alpha)}{P(\alpha)} + \frac{\mu_o w}{8\pi} \qquad (3.4.3)$$

Rewriting it in terms of the scale inductance and the dimensionless wire-length, the inductance is now given by

$$\frac{L_D}{L_o} = Nk \frac{S(\alpha)}{P(\alpha)} + \frac{k}{4} \qquad (3.4.4)$$

From equation (3.4.2) and the wire contact condition, b is eliminated and $\sin(\pi/N)$ is approximated by π/N, as in the previous cases, to give

$$N = \left(\frac{2\pi k}{P(\alpha)}\right)^{1/2} \qquad (3.4.5)$$

Back into equation (3.4.6), the full inductance is now given by

$$\frac{L_D}{L_o} \longrightarrow (2\pi)^{1/2} \cdot \frac{S(\alpha)}{P(\alpha)^{3/2}} k^{3/2} + \frac{k}{4} \qquad (3.4.6)$$

The inductance is maximised for a value of α that maximises $S(\alpha)/P(\alpha)^{3/2}$. This quantity is plotted in Fig. 3.12 against α using values obtained numerically by the computer program given in Appendix 1. The peak occurs for $\alpha = 5.3$, where $S(\alpha)/P(\alpha)^{3/2} = 0.1252$ and $P(\alpha) = 19.69$.

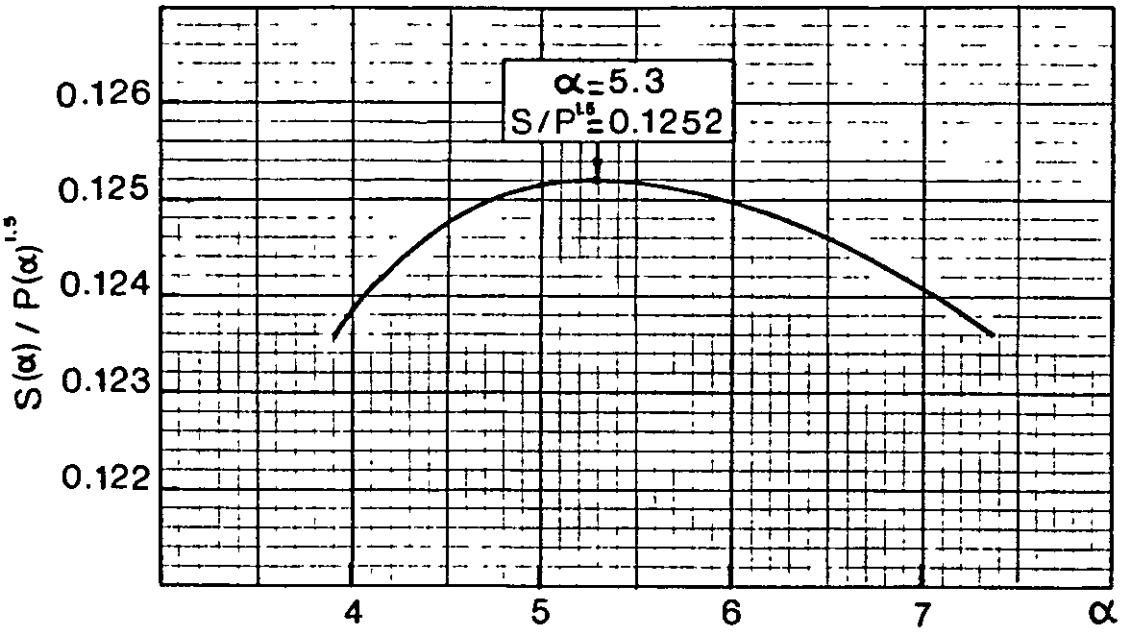

Fig. 3.12 Localisation of the optimum radius ratio of a D-shape cross-section toroid.

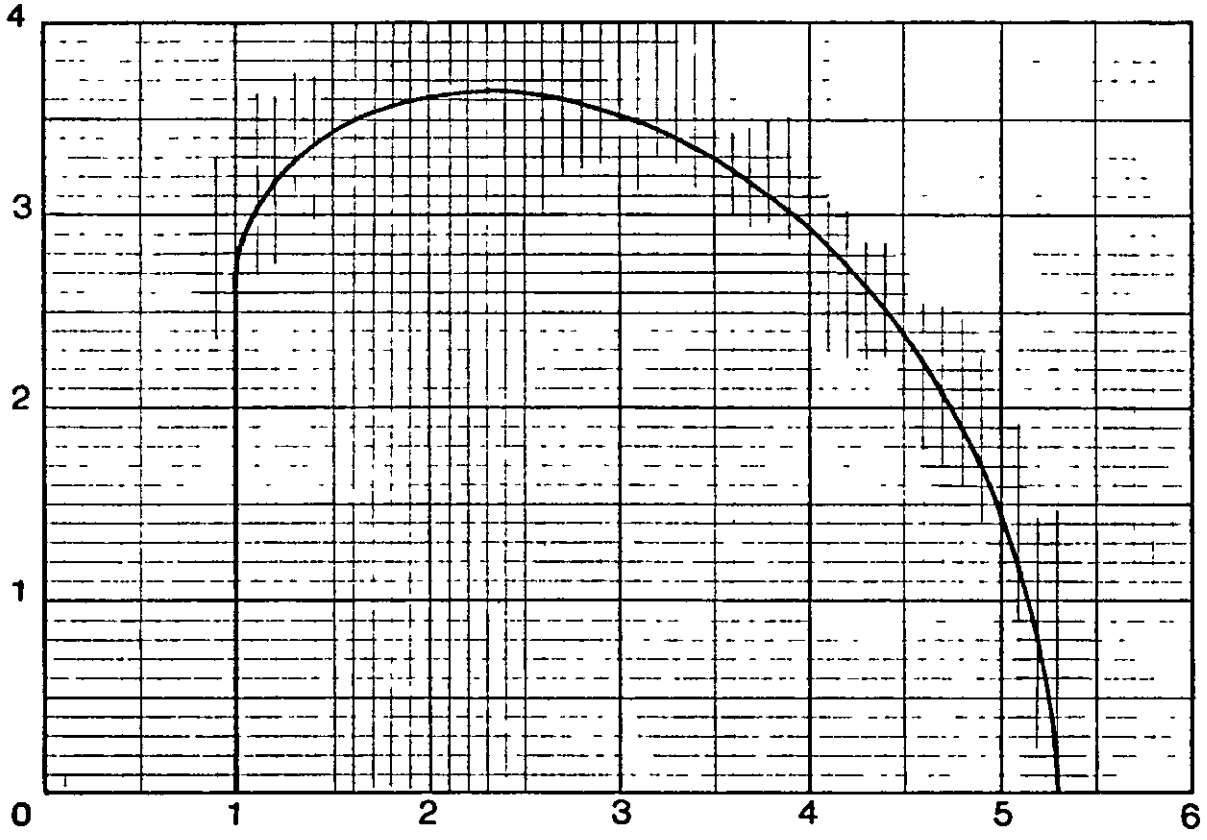

Fig. 3.13 The optimum single-layer toroid cross-section with $\alpha=5.3$

The optimum number of turns is thus given by

$$N = 0.5649\ k^{1/2} \qquad (3.4.7)$$

and the maximum inductance is

$$\frac{L_D}{L_o} = 0.3139\ k^{3/2} + 0.25\ k \qquad (3.4.8)$$

The D-shape corresponding to $\alpha = 5.3$ is plotted on a square grid in Fig. 3.13.

3.5 Comparison of Results

	Best inductance L/L_o	Optimum number of turns
Square section	$0.2522\ k^{3/2} + 0.25k$	$0.6329\ k^{1/2}$
Circular section	$0.2722\ k^{3/2} + 0.25\ k$	$0.8165\ k^{1/2}$
D-shape section	$0.3139\ k^{3/2} + 0.25\ k$	$0.5648\ k^{1/2}$

The above table shows that the inductance of the best D-shape toroid (comparing just the first term for large k) is about 15% better than the inductance of the best circle section toroid, which is 8% better than the inductance of the best square section toroid. The most economic single layer toroid is, therefore, a D-shape section toroid with radius ratio $\alpha = 5.3$. On the other hand the best D-shape toroid is seen to have fewer turns than the circular toroid, which means it is a bit more voluminous. A graph is given in Fig. 3.14 to help designing any of the three optimum toroids.

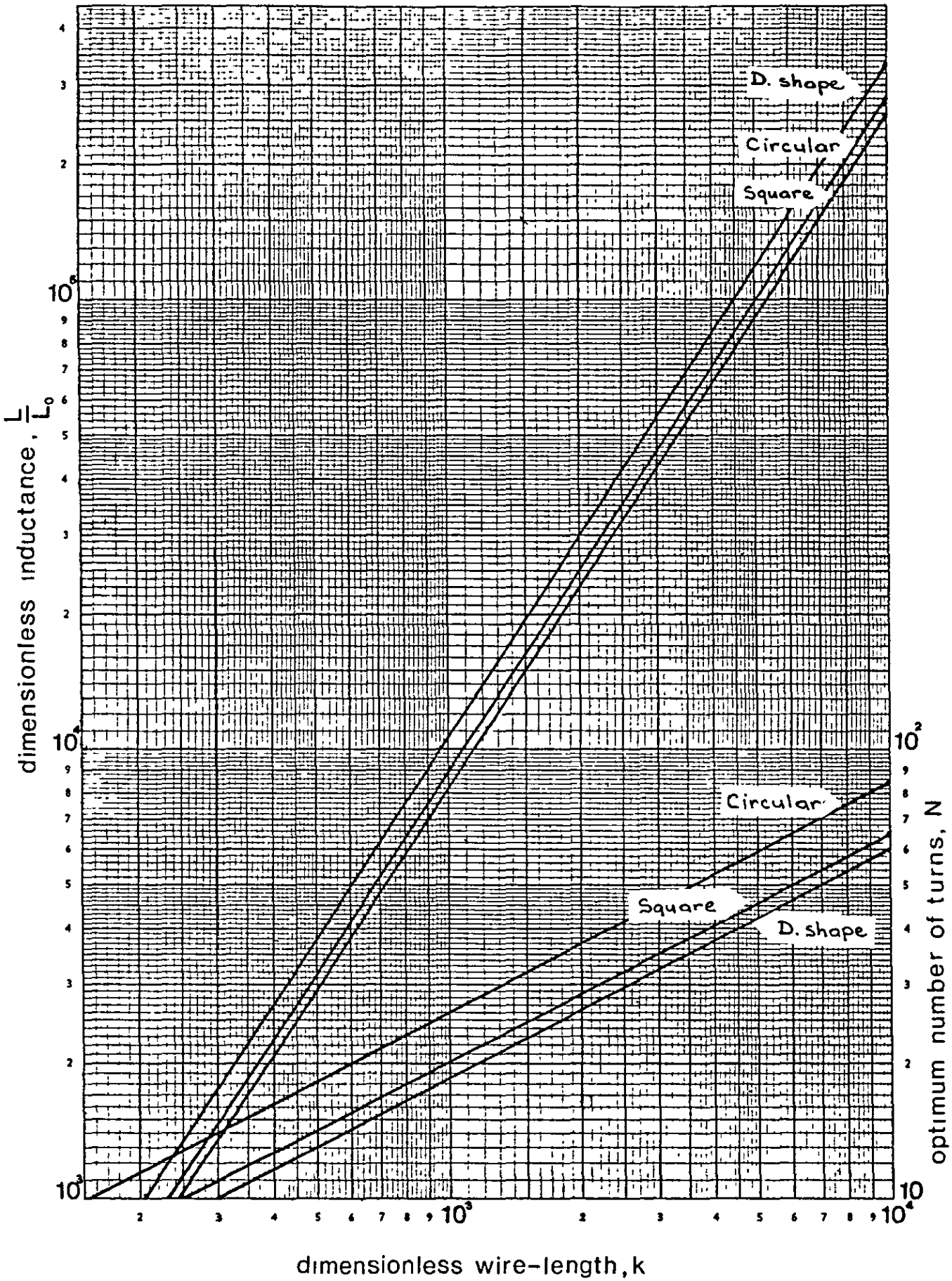

Fig. 3.14 Maximum inductance & optimum number of turns for single-layer air-cored toroidal inductors.

In practice it is not always possible to use the most economic design because it may not fit into the space allowed in the electronic system. Nevertheless, the previous study will help engineers, if space is not a problem, make the most economic design of single layer toroids without getting any inferior design by trial and error especially when the production is high. A direct application of these results has already found its way in the practical design of inductors for dI/dt limitation in a power electronics circuit [22].

The principal results of this chapter have been published [23] and a reprint of the paper appears in Appendix 4.

CHAPTER 4

THE D-SHAPE TOROIDAL CAGE INDUCTOR

4.1 Introduction

The development of new devices capable of controlling larger currents has made possible a rapid advance in power electronics. However, some difficulties are encountered with the passive components required for this technology. Inductors, in particular, sometimes present serious problems. As mentioned in Chapter 1, because of the high currents they carry, inductors (like solenoids, for example), generate high external magnetic fields that may interfere with nearby electronic equipment. Inductors can also have saturation problems if they are iron cored.

A good solution to these problems is the air cored toroidal inductor which is used in many power electronics circuits. Unfortuntely, this type of inductor has manufacturing problems at the present time and cost disadvantages, if compared to solenoids. Nevertheless, attempts are being carried out by specialists to overcome them and find optimum solutions.

One special air cored inductor, which has proved itself useful in high current power electronics, is the toroidal cage coil [7]. It is a robust component that was developed a few years ago at Brush Electrical Machines Ltd. and at

Loughborough University. The first cages were constructed with rectangular shaped windows and are used in thyristor choppers for railway traction drives. Good formulae for the inductance and power dissipation were derived and tested for this type of cage [7].

In the present work, a similar study is carried out for cages having the optimum D-shape of window. It will be shown in the last section of this chapter that this type of cage gives improved performance compared with the rectangular cage.

4.2 Construction of the Cage

As shown in Plate 1, a toroidal cage inductor is made by assembling six identical subcoils. They are joined together in a well defined way so that the complete structure looks like a six turns toroid. Each subcoil is wound separately on a special former using a winding machine or a slow running lathe.

The former, shown in Plate 2 and Fig. 4.1, consists of a central wooden board which is cut to shape using a bandsaw and a sander; the shape we are concerned with in this work is the D-shape treated in Chapter 2. In order to secure the winding against slipping, the central board is sandwiched between two wooden cheeks which are fixed to it by means of small bolts. Slots and windows are successively cut into the board and cheeks to allow for tapes to pass

Plate 1

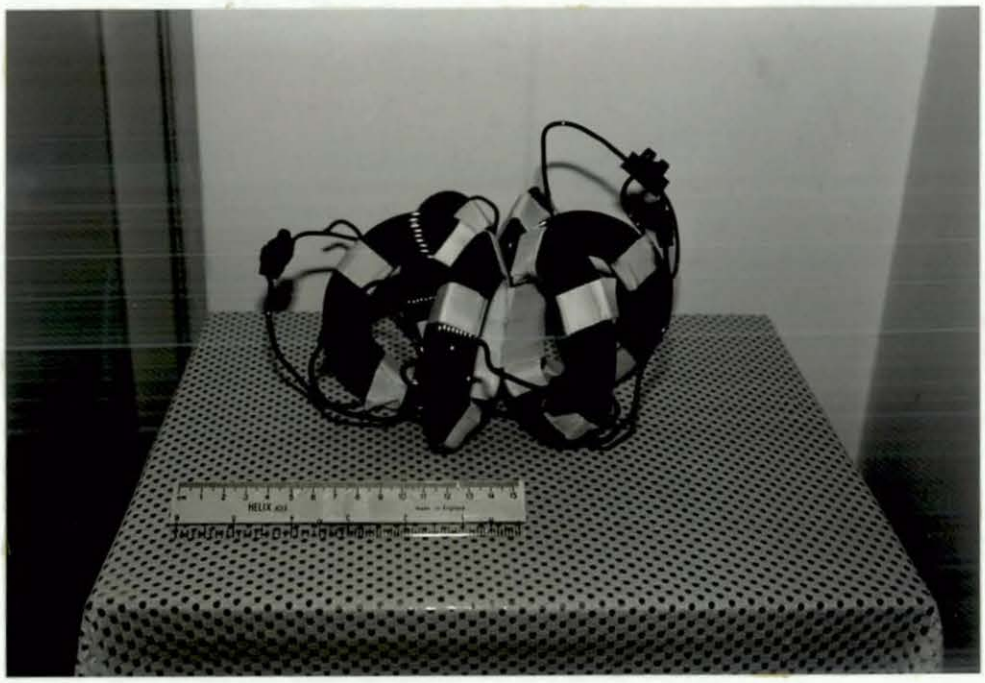

Plate 2

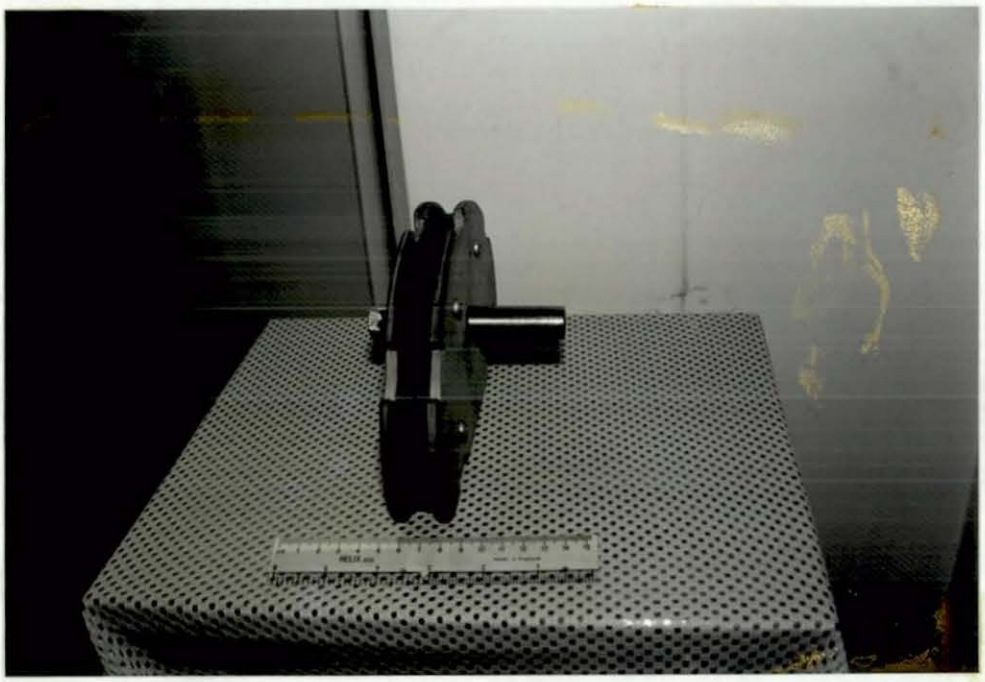

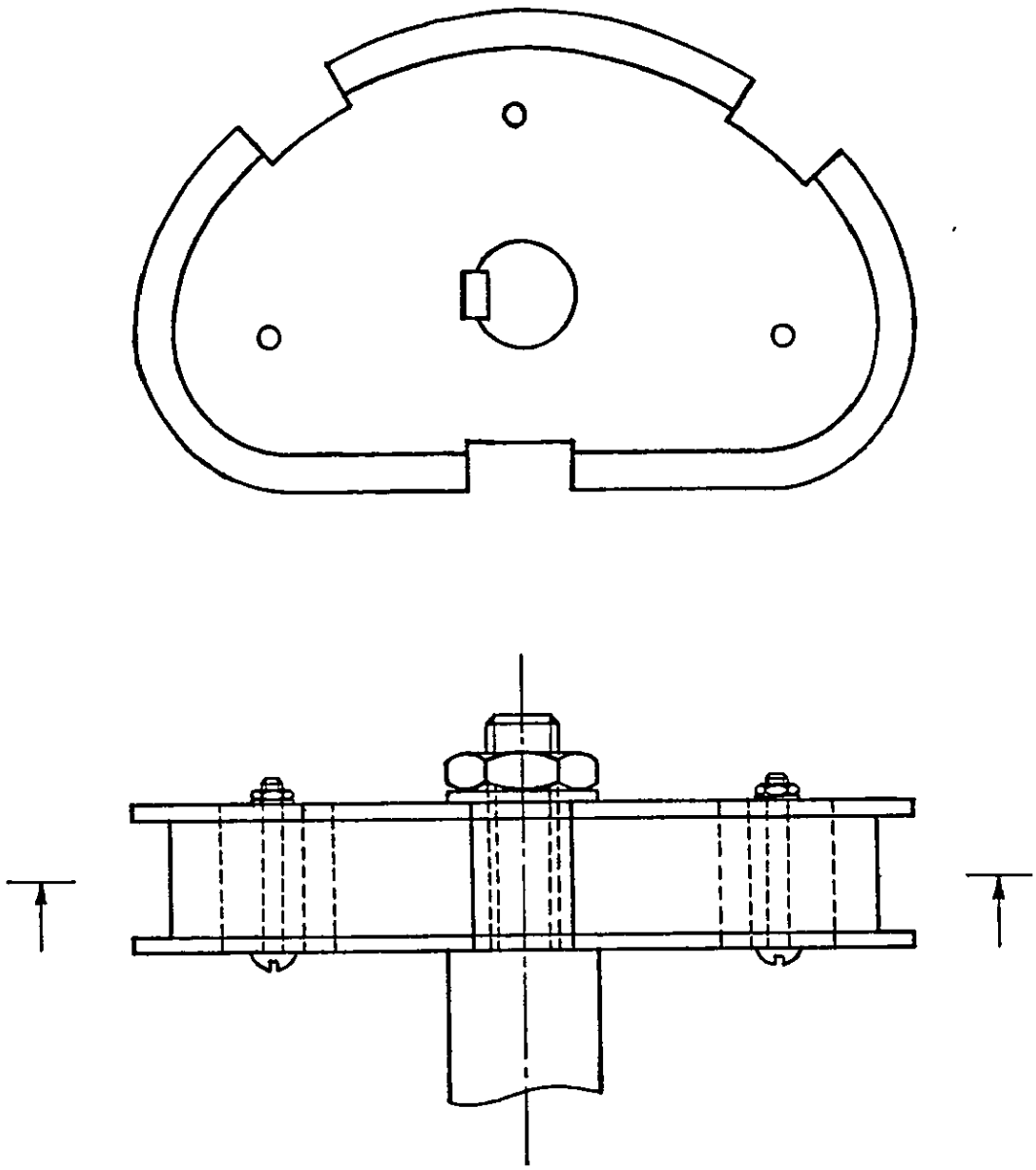

Fig. 4.1 Drawing of former with shaft

under and around the stack of wire, so as to prevent any collapse and facilitate the easy removal of the subcoil after the winding operation. A hub and a keyway are made at the centres of the central board and cheeks, then the thin threaded end of a metal shaft, with a key fixed on it, is passed through the former and secured with a big nut. Finally, the other end of the shaft is housed inside the mandrel of the winding machine and solid enamelled copper wire is wound onto the central board.

The first layer of the winding has n turns and covers the whole width of the central board which is given by

$$H = nd \tag{4.2.1}$$

where d is the diameter of the enamelled copper wire and n is given from the relation

$$N = 6 \sum_{i=1}^{n} i \tag{4.2.2}$$

or $$N = 3n\,(n + 1) \tag{4.2.3}$$

where N is the total number of turns of the cage.

Each of the following layers slotsinto the grooves of the layer below it and has thus one turn fewer. As shown in Fig. 4.2, all the layers, with the last one consisting of just one turn, constitute a regular pyramid.

The same process is repeated for the five other subcoils. In each one the wires form a bunch with an envelope section that is an equilateral triangle. As sketched in Fig. 4.3, when the six subcoils are joined together and bound with glass tape, the constructed cage has a solid central limb with an hexagonal envelope section.

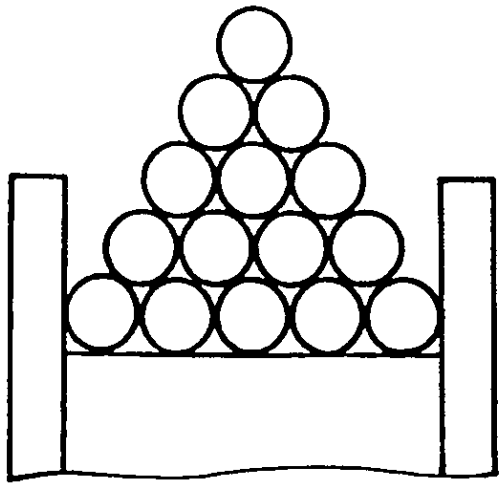

Fig. 4.2 Method of winding a subcoil

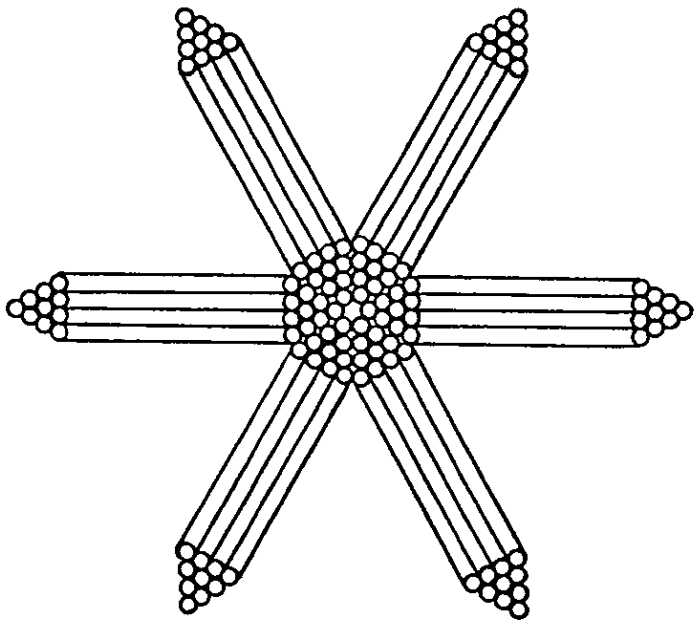

Fig. 4.3 Plan cross-section of cage inductor

To harden the structure and avoid short circuits the cage could be impregnated with liquid resin and heat treated. This technique is used for production coils at Brush Electrical Machines Ltd., but as similar facilities are not available at Loughborough University three of our prototypes were left without impregnation.

Different connections of the subcoils are possible. They could be

- Series-connected to give the greatest inductance.
- Paralleled in pairs and the pairs series-connected to give one quarter the inductance with twice the current rating.
- Paralleled in threes and the threes series-connected to give one ninth the inductance with three times the current rating.

4.3 Inductance Formula

In order to construct inductors with determined inductance and current rating values, it is necessary to have in hand accurate enough formulae from which the design parameters can be obtained. Inductance formulae of well known coils are available in many textbooks, but for special types they have to be derived theoretically and tested in practice.

In the case of the toroidal cage with rectangular window shape, for example, a working formula [7] was derived in terms of the geometry and the number of turns using the magnetic field energy method. A good agreement between theory and experiment was obtained.

That successful method is extended here to toroidal cages having the optimum D-shape of window. Similarly to the rectangular cage, the open hexagonal structure is approximated by a closed configuration, as shown in Fig. 4.4, so that circular field lines can be assumed and Ampere's theorem can be used. The D-shape is also divided into four regions in which the magnetic field is estimated separately. The energy is obtained from the expression of the magnetic field and the inductance is finally deduced.

The following calculations are done for a coil having N turns and carrying I amps.

Region (1): The toroidal air space

The inductance of this region, assumed perfectly toroidal, has the expression of the inductance of an ideal toroid having the same shape, but with the same number of turns as the complete cage. It is given in section 2.4 in terms of the inner radius b and the computed inductance $S(\alpha)$; and rewritten here

$$L_1 = \frac{\mu_o N^2}{2\pi} b\, S(\alpha) \qquad (4.3.1)$$

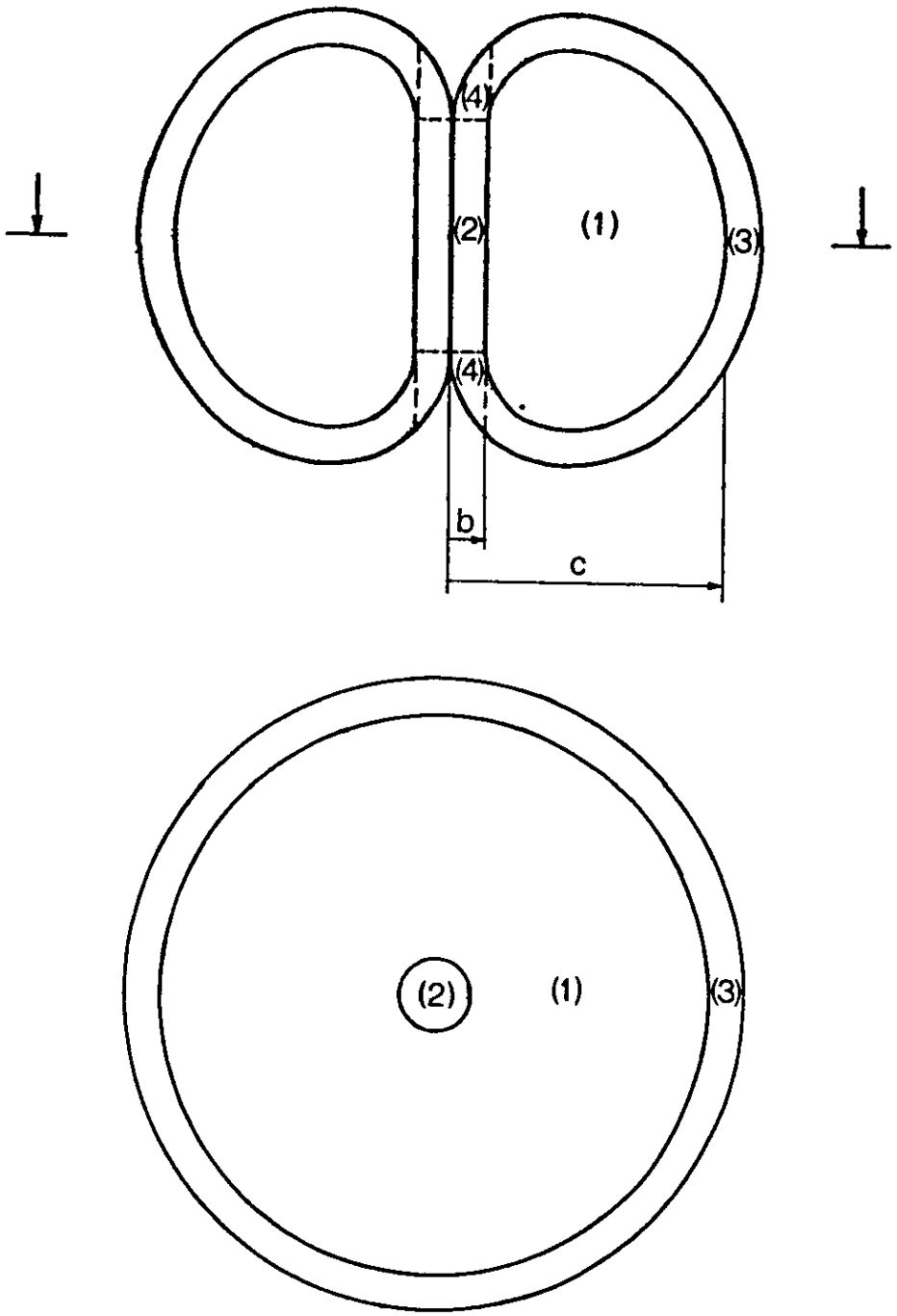

Fig. 4.4 Closed model for calculating the inductance

where α corresponds to the ratio of the outer to inner radius of the inner envelope or window of the coil.

Region (2): The central limb

Inside the central limb, assumed having a circular cross-section, the average magnetic field, at a radius r, is

$$B_2(r) = \frac{\mu_o NIr}{2\pi b^2} \tag{4.3.2}$$

The field energy in a limb of length l_c is then

$$W_2 = \int \frac{B_2^2(r)dV}{2\mu_o} \tag{4.3.3}$$

$$= \int_o^b \frac{\mu_o}{2} * \frac{NIr}{2\pi b^2} * l_c * 2\pi r dr \tag{4.3.4}$$

$$= \frac{\mu_o}{4\pi} \frac{N^2 I^2 l_c}{b^2} \left[\frac{r^4}{4}\right]_o^b \tag{4.3.5}$$

$$= \frac{\mu_o}{16\pi} N^2 I^2 l_c \tag{4.3.6}$$

and the internal inductance follows

$$L_2 = \frac{2W_2}{I^2} \tag{4.3.7}$$

$$= \frac{\mu_o N^2}{8\pi} lc \tag{4.3.8}$$

Using the relation $l_c = 2e = 2bE(\alpha)$, given in section 2.4, the above inductance expression becomes

$$L_2 = \frac{\mu_o N^2}{4\pi} bE(\alpha) \tag{4.3.9}$$

Region (3): The outer layer

Having two parallel envelopes, this region is bounded by the toroidal air space and the outside of the cage. The inner envelope has the optimum D-shape toroid geometry, but the outer has no simple analytical expression that may help to compute the inductance of the outer layer. The radius of curvature could be used, but it would lead to very complicated computations that are unnecessary because the contribution of the outer layer is not big, as will be seen later. The outer envelope is, therefore, approximated by the envelope of an optimum shape ideal toroid with radius ratio $\alpha + 1$.

In the rectangular cage the magnetic field was assumed [7] to fall linearly to zero across the two cylindrical zones at the top and bottom of the cages, so that the energy density would fall quadratically to zero into these regions. Since the mean of such a quadratically varying function is one third of the peak value, they were assigned the maximum energy for one third of their thickness.

This reasoning is used for the whole outer layer and its inductance is thus estimated by

$$L_3 = \frac{1}{3} \left[S(\alpha+1) - S(\alpha) \right] \frac{\mu_o N^2 b}{2\pi} \qquad (4.3.10)$$

Region (4): The corners layer

It is the small region containing the six small corners which are located between the central limb and the outer layer. Due to its difficult geometry and its very small contribution in the total inductance of the cage, it is dealt with by just arbitrarily adding a length b to the central limb.

$$L_4 = \frac{\mu_o N^2}{2\pi} \, b \qquad (4.3.11)$$

This crude procedure seems justified because even a large percentage error in a small part of the total energy cannot make a serious error in the whole.

Summing the contributions of the four regions yields the full inductance

$$L(b,\alpha) = \frac{\mu_o N^2 b}{2\pi} \left[\frac{2E(\alpha)+ 1}{4} + \frac{2}{3} S(\alpha)+ \frac{1}{3} S(\alpha+ 1) \right] \qquad (4.3.12)$$

$$= \frac{\mu_o N^2 b}{2\pi} T(\alpha) \qquad (4.3.13)$$

Values of $E(\alpha)$, $S(\alpha)$ and $S(\alpha+1)$ were obtained with the computer program in Appendix 1, and are given with $T(\alpha)$ in Table 4.1 for a range of values of α.

From that table it can be seen that the contribution of the outer layer is about 38% for $\alpha = 2$, 23% for $\alpha = 3$, 16% for

α	$E(\alpha)$	$S(\alpha)$	$S(\alpha+1)$	$\frac{2E(\alpha)+1}{4}$	$\frac{2}{3}S(\alpha)$	$\frac{1}{3}S(\alpha+1)$	$T(\alpha)$
2	0.2575	0.7191	2.7401	0.3787	0.4794	0.9134	1.7715
3	0.8469	2.7401	5.7561	0.6735	1.8267	1.9187	4.4189
4	1.5937	5.7561	9.6058	1.0468	3.8374	3.2019	8.0861
5	2.4527	9.6058	14.1663	1.4763	6.4039	4.7221	12.6023
6	3.3949	14.1663	19.3475	1.9479	9.4442	6.4493	17.8410
7	4.4024	19.3479	25.0819	2.4512	12.8986	8.3606	23.7104
8	5.4633	25.0819	31.3139	2.9816	16.7213	10.4380	30.1409
9	6.5692	31.3139	37.9999	3.5346	20.8759	12.6666	37.0771
10	7.7139	37.9999	45.1035	4.1069	25.3332	15.0345	44.4746

Table 4.1

$\alpha = 4$, and continues to increase for high values of α. With these results, one has to be careful in using the above inductance formula for low values of α. The formula has yet to be tested in practice, as it is in the next section, but it is possible to have boundaries for it first. We can say that for the lower limit the last two terms must be $S(\alpha)$, and for the upper limit they must be $S(\alpha + 1)$. In a more general way, the formula may be given by

$$L(b,\alpha,q) = \frac{\mu_o N^2 b}{2\pi}\left[\frac{2E(\alpha)+1}{4} + q\,S(\alpha) + (1-q)\,S(\alpha+1)\right] \qquad (4.3.14)$$

where q is a constant comprised between 0 and 1, and has to be determined experimentally.

4.4 Inductance Measurements

Five coils with different radius ratios and sizes (see Plate 3) have so far been prepared to test the general formula given by equation (4.3.14). Two of them were wound on a slow running lathe and the three others on a heavy duty winding machine made by Whitelegg of type CAW, as shown in Plate 4. During the winding operation the wires were kept in constant tension by a brake device which is added to the machine.

A Maxwell bridge arrangement, as shown in Fig. 4.5, was used for the inductance measurements. The voltage across the bridge was detected by an oscilloscope via an inter-

Plate 3

Plate 4

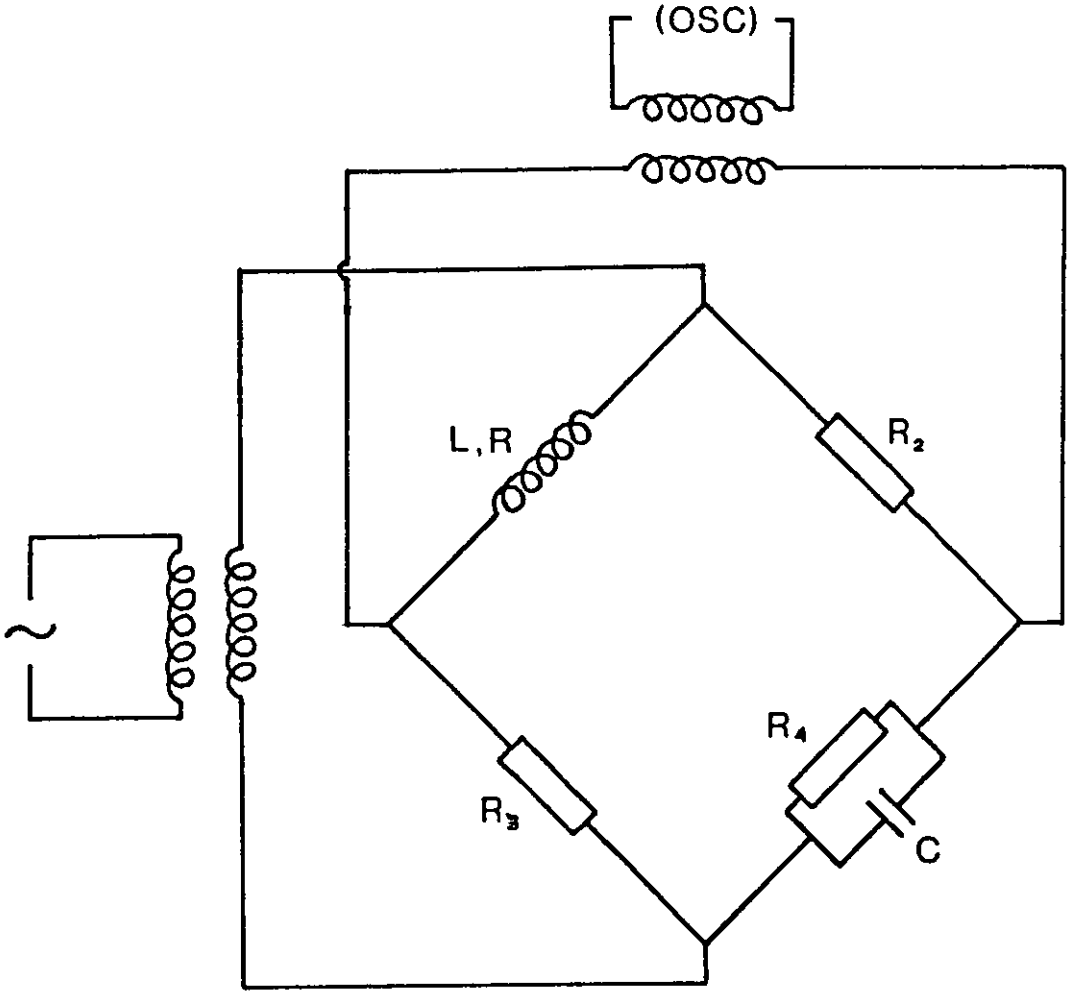

Condition of balance

$$R_2R_3 = (R + j L\omega)\ \frac{R}{1 + jC\omega R_4}$$

which implies

$$L = CR_2R_3$$

and

$$R = \frac{R_2R_3}{R_4}$$

Fig. 4.5 Maxwell Bridge

bridge transformer. The supply was also obtained via an interbridge transformer from an amplifier which was driven by a variable frequency sinusoidal oscillator.

The measurements were made for a range of power frequencies from 30 Hz to 3 kHz. As plotted in Fig. 4.6, in the low frequency band, which we are concerned with, the inductance has a constant value. For frequencies higher than 1 kHz, a decrease is observed. That fall of inductance is due to the creation of eddy currents which oppose the main current in the winding and result in some cancellation of parts of the magnetic field.

For calculation and practical purposes, the inner radius of the central limb, assumed circular, was approximated by the relation

$$b = nd \qquad (4.4.1)$$

where d is the diameter of the wire and n is the number of layers in each subcoil.

The measured values of the inductance are compared in Table 4.2 to values calculated from the formula given by equation (4.3.12) which corresponds to $q = \frac{2}{3}$ in equation (4.3.14). The corresponding values of $T(\alpha)$ are also compared in Fig. 4.7. For that specific value of q the agreement is very good and the error is reasonably small.

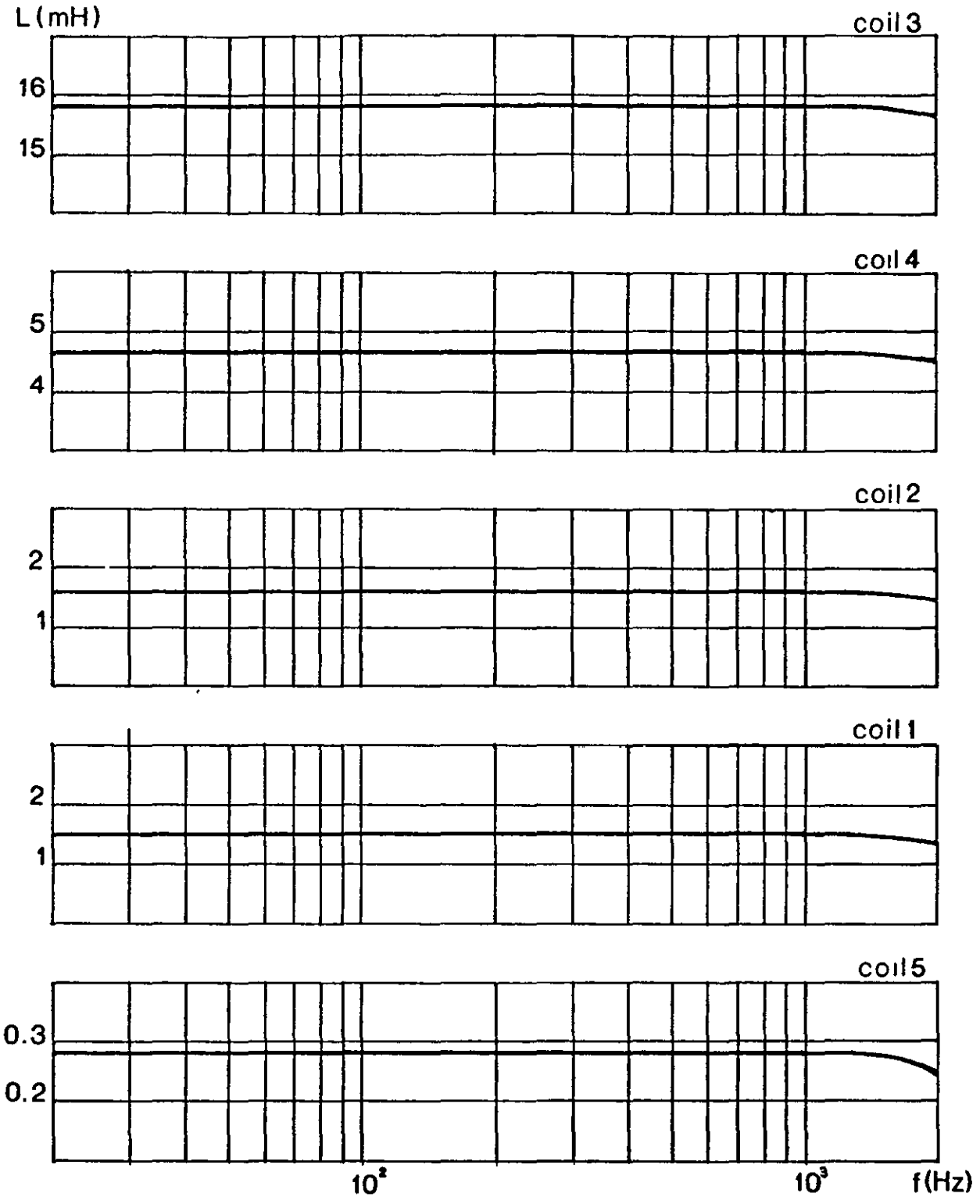

Fig. 4.6 Inductance against frequency

		Coil 1	Coil 2	Coil 3	Coil 4	Coil 5
	α	3	4	6	8	10
	d(mm)	2.6	2.6	2.6	2.0	2.0
	b(mm)	23.4	20.8	28.6	17.2	8.6
	N	270	216	396	216	60
	N^2	72900	46656	156816	46656	3600
	$T(\alpha)$	4.4189	8.0861	17.8410	30.1409	44.4746
L(mH)	Calc.	1.508	1.569	16.003	4.838	0.275
	meas.	1.490	1.595	15.970	4.660	0.280
	error(%)	+1.2	-1.6	+0.2	+3.8	-1.8

Table 4 2

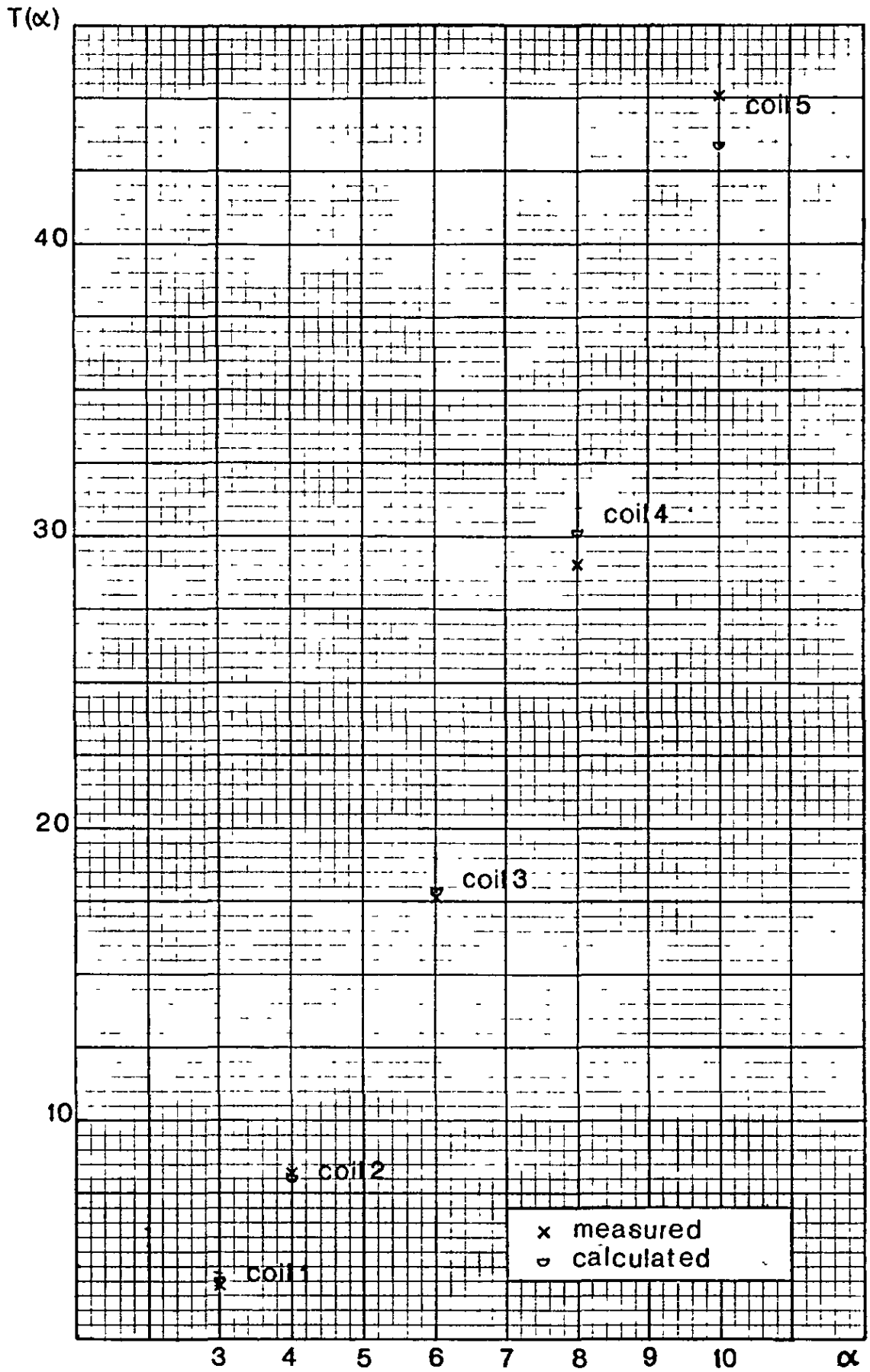

Fig. 4.7 Plot for comparing measured and calculated inductances

4.5 Effect of Field Ripples on the Inductance

The last line of Table 4.2 shows negative and positive signs for the error between the measured and calculated values of the inductance. This result is partly due to the approximation made to the outer envelope.

The derivation of the general inductance formula was made upon assuming a closed model in which the field lines are circular and we would have expected it to underestimate the measurements because the cage is made up of a small number of subcoils where the magnetic field has some ripples which raise up the energy; it could be explained as follows:

The magnetic field in a toroidal coil with a discrete number of subcoils is not totally confined inside. It may be given by

$$B_{\phi} = B_{av} + R \qquad (4.5.1)$$

where B_{av} is the average azimuthal field considered in the closed configuration and R is a field ripple which has zero line integral along any circular path having its centre on the coil axis.

In the expression for the energy, the magnetic field has the squared form

$$B_{\phi}^2 = B_{av}^2 + 2\, B_{av}\, R + R^2 \qquad (4.5.2)$$

The second term averages to zero, and we are left with the average field squared and a term which is always positive.

Indeed, this shows that the presence of ripples results in a higher inductance compared to the closed configuration.

To explain this reasoning experimentally, some measurements have been made with the cages having different numbers of subcoils. Table 4.3 shows that with just two symmetrical subcoils connected in series the inductance, which is proportional to the number of turns squared, is one fifth the inductance of the six subcoils connection instead of being one ninth. Also, with three subcoils it is one third instead of one fourth. These results imply that for a same number of turns the inductance of a two subcoils cage is higher than the inductance of one with three subcoils which is itself higher than the inductance of the six subcoils structure.

The effect of ripples is, therefore, greater as the number of subcoils is decreased. It is also obvious that it becomes negligible when the number of subcoils is highly increased because we will meet the closed configuration.

To show once more that the ripples have an effect on the inductance some other measurements have been made with other types of connections. The subcoils were paralleled in pairs with the pairs series connected, and then they were paralleled in threes with the threes series connected. As shown in Table 4.3, the inductances were respectively one quarter and one ninth the inductance of the six subcoils series connection. Thus it proves that

	Coil 1	Coil 2	Coil 3	Coil 4	Coil 5
L_6(mH)	1.490	1.595	15.970	4.660	0.280
L_3(mH)	0.506	0.540	5.300	1.560	0.090
L_2(mH)	0.308	0.320	3.100	0.920	0.055
L_6/L_3	2.95	2.95	3.01	2.99	3.11
L_6/L_2	4.84	4.98	5.15	5.06	5.09
$L_{3,2}$(mH)	0.373	0.400	3.99	1.170	0.070
$L_{2,3}$(mH)	0.165	0.180	1.750	0.500	0.030
$L_6/L_{3,2}$	4.00	3.99	4.00	3.98	4.00
$L_6/L_{2,3}$	9.03	8.86	9.13	9.32	9.33

L_6 — All six subcoils connected in series

L_3 — Just three subcoils connected in series

L_2 — Just two subcoils connected in series

$L_{3,2}$ — All six subcoils paralleled in pairs and the pairs series connected

$L_{2,3}$ — All six subcoils paralleled in three and the threes series connected

Table 4.3

the effect of the ripples was the same in the three cases, and it is so because all the six subcoils were present with these connections.

4.6 Loss Formulae

The ohmic and eddy current losses are the two major kinds of losses appearing in the windings of air cored inductors carrying time varying currents.

The ohmic loss is easily calculated by assuming the current density to be uniform in the cross-section of the wire. For N wires of radius a and conductivity σ, connected in series, it is given by

$$W_{dc} = R_{dc} I_o^2 \qquad (4.6.1)$$

with

$$R_{dc} = \frac{N\bar{l}}{\pi a^2 \sigma} \qquad (4.6.2)$$

where $\bar{l}$ is the mean turn length.

In the case of the D-shape toroidal cage, an expression for the mean turn length is derived in Appendix 3; that is

$$\bar{l} = 2b\,(E + P_1 A + P_2 B) \qquad (4.6.3)$$

with

$$A = 1 + (1 - \frac{1}{n}) \frac{1}{\sqrt{3}(\sqrt{\alpha} - 1 + z_m - E)} \qquad (4.6.4)$$

and

$$B = 1 + (1 - \frac{1}{n}) \frac{1}{\sqrt{3}(\alpha - \sqrt{\alpha} + z_m)} \qquad (4.6.5)$$

P_1, P_2, Z_m can be obtained with the computer program given in Appendix 1.

With alternating currents, the magnetic field induces eddy currents which oppose the main current. These small currents result in a non-uniformity of the current density and thus an effective increase of the resistance.

Two types of eddy currents participate in the losses. The first is due to the proximity effect which is the induction of currents in each wire by the magnetic field of the other conductors. The second is the skin effect which is caused by the magnetic field of that same conductor.

At low frequencies, the contribution of the skin effect loss in bunches of wires is negligible compared to the proximity effect loss [1]. Thus it is not considered in the formulation of the loss for the cage.

The peak power loss per unit length in a round conductor of radius a, situated in a uniform transverse alternating field $B_o \cos\omega t$, is given by [24]

$$W_1 = \frac{\pi}{4} a^4 B_o^2 \omega^2 \sigma \qquad (4.6.6)$$

For a circular bunch of radius b and composed of N wires, each one carrying the same current, the magnetic field at a radius $r \leqslant b$ is given by

$$B(r) = \frac{\mu_o N I_o r}{2\pi b^2} \qquad (4.6.7)$$

Provided N is large enough, the average density of wires per unit area is $N/\pi b^2$. Taking the annulus between r and r + dr, the loss in the bunch, using equations (4.6.6) and (4.6.7), is

$$W_E = \int_o^b W_1 \frac{N}{\pi b^2} \, 2\pi r \, dr \qquad (4.6.8)$$

$$= \int_o^b \frac{\sigma a^4 \omega^2 I^2 N^3 \mu_o^2}{16 \pi b^6} \, r^3 \, dr \qquad (4.6.9)$$

$$= \frac{1}{32\pi} \frac{\mu_o^2 \sigma \omega^2 I_o^2 N^3 a^4}{b^2} \qquad (4.6.10)$$

In a recent work, Murgatroyd [25] showed that the proximity effect loss in a bunch of wires of any given envelope section shape may be expressed as a function of the proximity effect loss in a circular envelope bundle having the same number of turns. The relation is

$$W = \lambda W_E \qquad (4.6.11)$$

where λ is a factor which depends on the envelope section shape and the number of wires. In the case of the cage, it is referred to as λ_h for the hexagonal bunch and λ_t for the triangular bunch.

The loss in the central limb, which is an hexagonal envelope section bundle of N wires of length l_c, is

$$W_h = \lambda_h W_E l_c \qquad (4.6.12)$$

The loss in each outer limb, having a number N/6 of turns and a length $(\bar{l}-l_c)$, is

$$W_t = \lambda_t W_E'(\bar{l} - l_c) \tag{4.6.13}$$

Replacing b^2 by $b^2/6$ and N by $\frac{N}{6}$ in equation (4.6.7)

$$W_E' = \frac{1}{32\pi} \frac{\mu_o^2 \sigma \omega^2 I_o^2 (N/6)^3 a^4}{b^2/6} \tag{4.6.14}$$

$$= \frac{1}{32\pi} \frac{\mu_o^2 \sigma \omega^2 I_o^2 N^3 a^4}{36\, b^2} \tag{4.6.15}$$

which implies

$$W_t = \lambda_t \frac{W_E}{36} (\bar{l} - l_c) \tag{4.6.16}$$

The loss in the six outer limbs is thus given by

$$6\, W_t = \lambda_t \frac{W_E}{6} (\bar{l} - l_c) \tag{4.6.17}$$

The total eddy current loss in the cage is then

$$W_h + 6W_t = W_E [\lambda_h l_c + \frac{\lambda_t}{6} (\bar{l} - l_c) \tag{4.6.18}$$

The ratio of effective a.c resistance to d.c resistance is given by

$$\frac{R_{ac}}{R_{dc}} = \frac{W_{dc} + W_h + 6\, W_t}{W_{dc}} \tag{4.6.19}$$

Introducing the parameter p defined by

$$p = \lambda_h \frac{l_c}{\bar{l}} + \frac{\lambda_t}{6} (1 - \frac{l_c}{\bar{l}}) \tag{4.6.20}$$

yields

$$\frac{R_{ac}}{R_{dc}} = 1 + \frac{W_E}{W_{dc}} \bar{l} p \tag{4.6.21}$$

In terms of the frequency and using equations (4.6.1) and (4.6.10) it becomes

$$\frac{R_{ac}}{R_{dc}} = 1 + Sf^2 \qquad (4.6.22)$$

where

$$S = \frac{2\pi^4}{10^{14}} \frac{a^6 \sigma^2 N^2}{b^2} p \qquad (4.6.23)$$

The value of the permitivity is $\mu_o = 4\pi \times 10^{-7}$ H/m

The above theory was derived with straight isolated bunches which are situated in their own magnetic field. In the toroidal cage, the bunches have curved parts and are affected by each others magnetic field. Therefore, a measurement based correction has to be made to the constant S which becomes

$$S_c = \varepsilon S \qquad (4.6.24)$$

where ε is a correction factor that will be determined experimentally in the next section.

4.7 Resistance Measurements

The direct current resistances of the five coils were measured by Kelvin bridge and compared to the values calculated from equation (4.6.2) in which the resistivity of copper was taken to be 1.682×10^{-8} ohm m. Table 4.4 shows that the agreement is very good despite the approximation

	Coil 1	Coil 2	Coil 3	Coil 4	Coil 5
α	3	4	6	8	10
n	9	8	11	8	4
N	270	216	396	216	60
E	0.8469	1.5937	3.3949	5.4633	7.7139
Z_m	1.4625	2.4000	4.4950	6.7916	9.2318
P_1	1.0622	1.4262	2.0183	2.5041	2.9244
P_2	2.1366	3.4433	6.2978	9.3667	12.5850
A	1.3808	1.2797	1.2059	1.1600	1.1177
B	1.1880	1.1148	1.0652	1.0422	1.0270
b(mm)	23.4	20.8	28.6	17.2	8.6
a(mm)	1.25	1.25	1.25	1.00	1.00
$\bar{l}$(mm)	227.1	301.9	717.1	623.7	411.2
R_{dc} (ohm) Calc.	0.210	0.223	0.973	0.721	0.132
R_{dc} (ohm) Meas.	0.221	0.232	0.954	0.694	0.135
error(%)	-5.0	-3.9	+2.0	+3.9	+2.2

Table 4.4

made to obtain the total length of wire of the cage.

On the other hand, the a.c resistances were obtained for a range of low frequencies in the Maxwell bridge used for the measurements of the inductance. Similarly to the theory, the linear dependence of the a.c resistance on squared frequency is observed, as shown in Fig. 4.8.

From the plot given in Fig. 4.8, the values of the constant S were obtained and compared in Table 4.5 to the values calculated from equation (4.6.23). As mentioned in the previous section, the agreement is not good and a correction has to be made. However, the way the results have come out for α large was not as predicted. Acarnley and Danbury [26] have shown that the loss in bunches of wires is minimal if the field lines are circular, so we would have expected the measurement to underestimate the theory.

. The calculation was performed for isolated straight bunches made with fine wires while the cage is comparatively made with thick wires and has a far more complex geometry. Nevertheless a very interesting result was obtained. The plot in Fig. 4.9 shows that the error on S increases almost linearly with α. Thus the correction factor is easily obtained graphically. The error on S is

$$\frac{S_{calc} - S_{meas}}{S_{meas}} = \frac{\alpha - 6}{10} \qquad (4.7.1)$$

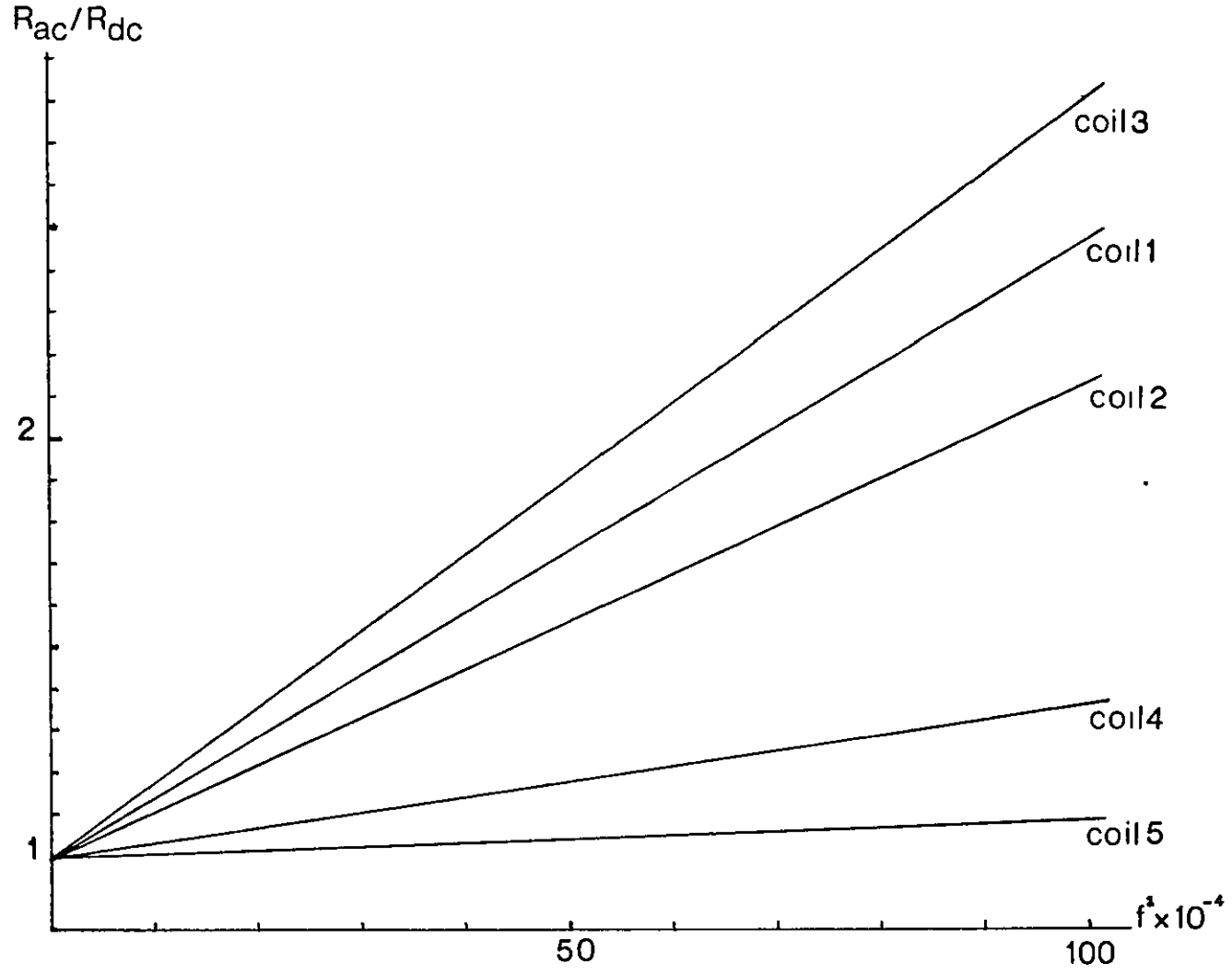

Fig 4.8 Resistance against frequency squared

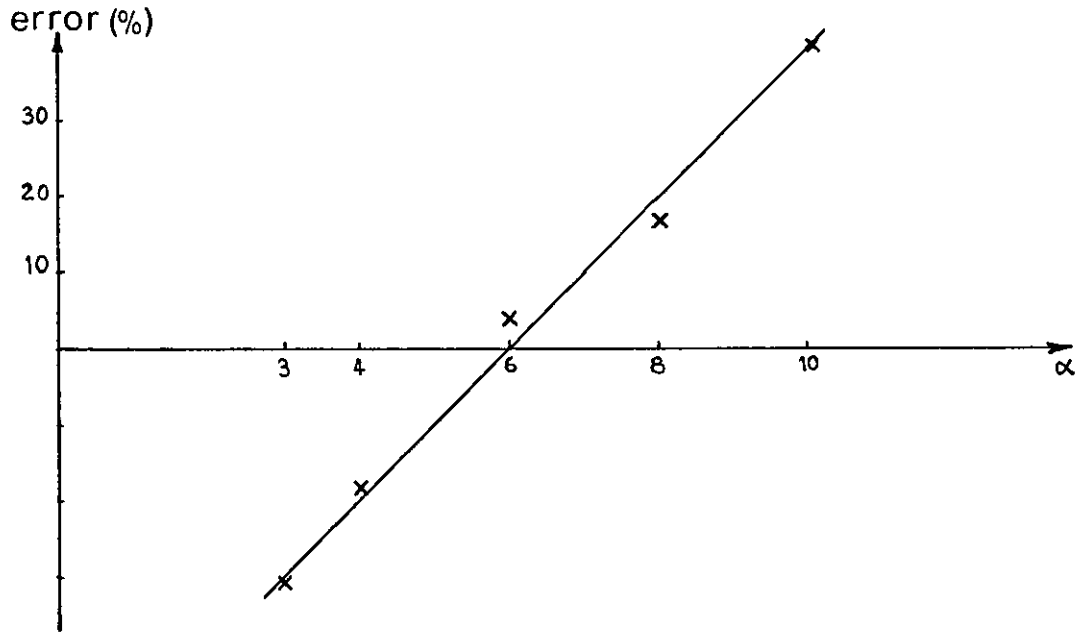

Fig. 4.9 Error on S

		Coil 1	Coil 2	Coil 3	Coil 4	Coil 5
	α	3	4	6	8	10
	a(mm)	1.25	1.25	1.25	1.00	1.00
	b(mm)	23.4	20.8	28.6	17.2	8.6
	N	270	216	396	216	60
	l_c(mm)	39.6	66.3	194.2	187.9	132.7
	$\bar{l}$(mm)	227.1	301.9	717.1	623.7	411.2
	k_h	0.990	0.988	0.993	0.988	0.973
	λ_t	0.856	0.850	0.865	0.850	0.774
	p	0.291	0.328	0.374	0.397	0.401
S ($\times 10^{-5}$ Hz^{-2})	Calc.	1.016	0.929	1.884	0.431	0.134
	Meas.	1.471	1.134	1.811	0.369	0.096
error (%)		-30.9	-18.1	+4.0	+16.8	+39.6
S_c ($\times 10^{-6}$ Hz^{-2})		1.451	1.161	1.884	0.359	0.096
error (%)		-1.4	+2.4	+4.0	-2.7	0.0

Table 4 5

which implies

$$S_{cal} = \frac{\alpha + 4}{10} \; S_{meas} \qquad (4.7.2)$$

Equating corrected and measured S yields

$$S_c = \frac{10}{\alpha + 4} \; S_{cal} \qquad (4.7.3)$$

and equation (4.6.22) becomes

$$\frac{R_{ac}}{R_{dc}} = 1 + \xi Sf^2 \qquad (4.7.4)$$

with

$$\xi = \frac{10}{\alpha + 4} \qquad (4.7.5)$$

The error on S_c is given at the bottom of Table 4.5 showing a better agreement.

4.8 Optimum Designs

The inductance of a toroidal cage coil of any cross-section shape may be given by

$$L = \frac{\mu_o}{2\pi} N^2 b F(\alpha) \qquad (4.8.1)$$

where b is the inner radius defined previously and $F(\alpha)$ is a dimensionless quantity which depends on the window shape.

The wire length of the cage may be given by

$$l = b \; N \; G \; (\alpha) \qquad (4.8.2)$$

where $G(\alpha)$ is the dimensionless mean turn perimeter.

The proportion of the central bunch cross-sectional area which is metal conductor may be defined as

$$\zeta = \frac{Nd^2}{b^2} \qquad (4.8.3)$$

where d is the diameter of the wire.

From the last two equations, b can be eliminated to give the number of turns

$$N = \zeta^{1/3} \left(\frac{ld}{G(\alpha)}\right)^{2/3} \qquad (4.8.4)$$

The inductance is now given by

$$L = \frac{\mu_o}{2\pi} \frac{\zeta^{1/3}}{d^{2/3}} l^{5/3} \frac{F(\alpha)}{G^{5/3}(\alpha)} \qquad (4.8.5)$$

In terms of the scale inductance $L_o = \frac{\mu_o d}{2\pi}$ and the dimensionless wire-length $k = \frac{l}{d}$, it becomes

$$\frac{L}{L_o} = \zeta^{1/3} \frac{F(\alpha)}{G^{5/3}(\alpha)} k^{5/3} \qquad (4.8.6)$$

$$= R\, k^{5/3} \qquad (4.8.7)$$

where R is a dimensionless coefficient which depends on the geometry of the cage.

The value of R was calculated from Table 4.2 and 4.4 for the five coils prepared in this work, and is compared to

the value of seven other coils with rectangular shape of window calculated from reference [7]. The tabulation below shows that the D-shape cages give better performance compared with the rectangular cages, except for large values of α. The D-shape advantage is lost for α large, because in this case the coils are voluminous and therefore have relatively fewer turns. Better designs are thus for low values of α.

D-shape cages

	Coil 1	Coil 2	Coil 3	Coil 4	Coil 5
R	0.148	0.143	0.123	0.110	0.112

rectangular cages

	Coil 1	Coil 2	Coil 3	Coil 4	Coil 5	Coil 6	Coil 7
R	0.111	0.113	0.083	0.111	0.103	0.096	0.107

CHAPTER 5

CONCLUSION AND SUGGESTIONS

This thesis has been mainly concerned with some optimum designs for air cored toroidal inductors. The calculation of the cross-section of a toroidal air cored inductor that has maximum inductance for a given d.c resistance was reviewed in Chapter 2. Mathematical methods were implemented in the computer program, given in Appendix 1, to obtain the plot of the optimum shape, the inductance of the toroid, and the perimeter of the cross-section. The program could be used with any work involving optimum D-shapes, as it was throughout this thesis.

In Chapter 3, Maxwell's problem of winding the greatest inductance for a given length of wire was solved for single layer toroidal coils with square, circular and D-shape cross-sections. The results are summarised in Fig. 3.14, so that the most economical design for any required inductance and current rating may be achieved using a simple graphical procedure.

Inductance and loss formulae were derived and tested for cages which exploit the D-shape profile, as shown in Chapter 4. A comparison with rectangular cages shows that this type of cage offers improvements in both manufacture and performance. The practical feature is that the D-shape has no corners and the wires are easily wound on the

former, whereas with rectangular shapes the wires cannot follow the right angle turns of the former, but bulge from it. The examination of the economic advantage was based on some practical results. It was shown in the last section of Chapter 4 that better values of R were obtained for D-shape cages with low values of α. Since the five thirds dependence of the inductance on the wire-length is true for cages with any given cross-section shapes, it is obvious that the most economical design is one which corresponds to the highest possible value of R.

As far as D-shape cages are concerned, further calculations could be made to find the optimum radius ratio α using equations (4.3.14) and (4.6.3). First investigations that have not been included in this thesis, using equation (4.3.12) which corresponds to $q = \frac{2}{3}$ in equation (4.3.14), have shown that the inductance decreases with α. Due to the approximation made to the outer envelope of the cage and because the inductance has a soft optimum no peak was obtained. However if more coils with low values of α are constructed and a better value of q is determined giving a much more accurate formula, a peak may probably occur.

REFERENCES

1. WELSBY, V.G.: 'The theory and design of inductance coils', Macdonald, London, 1960.

2. GROVER, F.W.: 'Inductance calculations', Dover Publications, New York, 1946.

3. BUKSTEIN, E.J.: 'Understanding transformers and coils', Foulsham & Co.Ltd., England, 1965.

4. COULON, F.De, JUFER, M.: 'Introduction a l'electrotechnique' Dunod, France, 1981.

5. LANDER, C.W.: 'Power electronics', McGraw-Hill, UK Ltd. 1981.

6. VAUFROUARD, B.: 'A manufacturers view on manufacturing & marketing toroidal transformers', Coil Winding International, England, August, 1985.

7. MURGATROYD, P.N., FARRER, W., HODGKINSON, R.P.D. and McLOUGHLIN, P.D.: 'The toroidal cage coil', IEE Proc. B, Elec.Power Appl., 1980, 127, (4), pp.207-214.

8. LEITES, L.V.: 'A coreless toroidal reactor for power systems', Elektrichestvo, 1960, 11, pp.556-568.

9. FILE, J., MILLS, R.G., and SHEFFIELD, G.V.: 'Large superconducting magnet designs for fusion reactors', IEEE Trans., 1971, NS-18, pp.277-282.

10. SHAFRANOV, V.D.: 'Optimum shape of a toroidal solenoid', Soviet Physics-Technical Physics, 1973, 17, pp.1433-1437.

11. MURGATROYD, P.N.: 'Some optimum shapes for toroidal inductors', IEE Proc.B., Electr.Power Appl., 1982, 129, pp.168-176.

12. GELFAND, I.M. FOMIN, S.V.: 'Calculus of variations', Prentice-Hall Inc., New Jersey, 1963.

13. WILSON, M.N.: 'Superconducting Magnets', Oxford University Press, New York, 1983.

14. MURGATROYD, P.N.: 'Variational methods notes', Electrical Dept., Loughborough University, 1986.

15. CAUNT, G.W.: 'Infinitesimal calculus', Oxford University Press, G.B., 1931.

16. GOODMAN, L.E., WARNER, W.H.: 'Dynamics', Wadsworth Publishing Company Inc., California, 1963.

17. GRALNICK, S.L., TENNEY, F.H.:'Analytical solution of the toroidal constant tension solenoid', Proceedings of the sixth symposium on engineering problems of fusion research, San Diego, CA., USA, 1975.

18. HOSKING, R.J., JOYCE, D.C., TURNER, J.C.: 'Numerical analysis', Hodder & Stoughton, 1978.

19. MAXWELL, J.C.: 'A treatise on electricity and magnetism. Volume 2', Oxford 1892.

20. SHAWCROSS, R.E., WELLS, R.I.: 'On the form of coil to give maximum self-inductance for a given length and thickness of wire', The Electrician, April 1915, 16, p.64.

21. BROOKS, B.: 'Design of standards of inductance, and the proposed use of model reactors in the design of air-core and iron-core reactors', Research Paper 342, Bureau of Standard J.Res., 1931, 7, pp.289-328.

22. TOUFIQ, M.L.: 'Private communication'.

23. MURGATROYD, P.N., BELAHRACHE, D.: 'Economic designs for single layer toroidal inductors', IEE Proc.B., Elect.Power Appl., 1985, 132, 6, pp.315-318.

24. CARTER, G.W.: 'The electromagnetic field in its engineering aspects', Longman, 1967.

25. MURGATROYD, P.N.: 'Calculation of proximity losses in multistranded conductor bundles', To be published.

26. DANBURY, R., ACARNLEY, P.: 'Losses in motor windings with switched excitation', IEE Conference Publication 254, Sept. 1985, pp.148-151.

APPENDIX 1

THE D-SHAPE COMPUTER PROGRAM

The program given in this appendix is written in Fortran 77, and was run on the Multics computer of Loughborough University. All quantities are reduced to dimensionless forms and depend on the radius ratio α. At the beginning of the program we can see three external functions which correspond to the first, second and third derivatives of the curve which defines the optimum D-shape. The second and third derivatives were added so that Taylor's expansion could be used with a good enough precision at the ends of the range where the slope is infinite. The number of steps chosen is 500, which is reasonably good for the Runge-Kutta and the trapezoidal method to give precise enough results. The input-output quantities are:

Input:

Alpha —— corresponds to the radius ratio $\alpha = b/c$

Output:

curv1 —— a file giving the upper curved part of the D-shape

curv2 —— a file giving the lower curved part of the D-shape

curv3 —— a file giving the straight leg at the inner radius

E —— corresponds to the length $E(\alpha)$ at the inner radius

Zm —— corresponds to the maximum height of the curve

S —— corresponds to the dimensionless inductance $S(\alpha)$

P —— corresponds to the dimensionless perimeter $P(\alpha)$

PP1 —— corresponds to the length $P_1(\alpha)$ between 1 and $\sqrt{\alpha}$

PP2 —— corresponds to the length $P_2(\alpha)$ between $\sqrt{\alpha}$ and α

```
      F(R)=ALOG(SQRT(R1*R2)/R)/SQRT(ALOG(R/R1)*ALOG(R2/R))
      G(R)=((ALOG(R/R1)*ALOG(R/R2))-(ALOG(R/SQRT(R1*R2))**R))/(R*
     1(ALOG(R/R1)*ALOG(R2/R))**1.5)
      V(R)=((ALOG(R/R1)*ALOG(R2/R))+((ALOG(SQRT(R1*R2)/R))**2))*
     1((ALOG(R/R1)*ALOG(R2/R))+(3*ALOG(SQRT(R1*R2)/R)))/((R**2)*
     1((ALOG/R/R1)*ALOG(R2/R))**2.5))
      open(unit=6,file='curv1',form='formatted')
      open(unit=7,file='curv2',form='formatted')
      open(unit=8,file='curv3',form='formatted')
      print*,'give Alpha'
      read(0,*)Alpha
      R1=10.
      R2=Alpha*R1
      H=.005
      Z=0.
      write(6,10)
      write(7,10)
      write(8,10)
   10 format(17X),'r',17X,'z'/)
      C1=Z/R2
      D1=Z
      RR=R2/R1
      ZZ=Z/R1
      write(6,20)RR,ZZ
      write(7,20)RR,ZZ
   20 format(F20.3,F20.7)
      R=R2-H
      Z+Z-H*F(R)-(XH**2)/2)/2)*H(R)-((H**3)/6)*V(R)
      C2=Z/R
      D2=Z
      EL=((C1+C2)/2)*H
      FL=SQRT((D2-D1)**2+H**2)
      C1=C2
      D1=D2
      I=IFIX(R/H)
      J=IFIX((R1+2*H)/H)
      K=-1
      ZMAX=Z
      do 100 IR=I,J,K
      R=IR*H
      P1=F(R)
      P2=F(R-0.5*H)
      P3=F(R-H)
      Z=Z-H*(P1+4*P2+P3)/6
      if (Z.gt.ZMAX) then
      ZMAX=Z
      FLM=FL
      end if
      X=R-H
      A=X-int(X)
```

```
      RR=M/R1
      ZZ+Z/R1
      OZ=(-1)*ZZ
      if (A.eq.0.) then
      write (6,20)RR,ZZ
      write(7,20)RR,OZ
      end if
      C2=Z/X
      D2=Z
      EL=EL+(((C2+C1)/2)*H)
      FL=FL+SQRT((D2-D1)**2+H**2)
      C1=C2
      D1=D2
  100 continue
      Z=Z-H*F(R1+H)+((H**2)/2)*G(R1+H)-((H**3)/6)*Y(R1+H)
      X=X-H
      RR=X/R1
      ZZ=Z/R1
      OZ=(-1)*ZZ
      write(6,20)RR,ZZ
      write(7,20)RR,OZ
      write(8,20)RR,ZZ
      write(8,20)RR,OZ
      write(0,105)Alpha
  105 format(13X,'Alpha='1X,F8.3)
      E=Z/R1
      write(0,110)E
  110 format(17X,'E=',1X/F12.7)
      zm=ZMAX/R1
      write(0,150) zm
  150 format (16X,'zm=',1X,F12.7)
      C2=Z/X
      D2=Z
      EL=EL+(((C2+C1)/2)*H)
      FL=FL+SQRT((D2-D1)**2+H**2)+D2
      S=(2*EL)/R1
      P=(2*FL)/R1
      write(0,200)S
  200 format(17X,'S=',1X,F12.7)
      write(0,300)P
  300 format(17X,'P=',1X,F12.7)
      PP2=FLM/R1
      PP1=FL/R1-(E+PP2)
      write(0,400)PP1
  400 format(15X,'PP1=',1X,F12.7)
      write(0,500)PP2
  500 format(15X,'PP2=',1X,F12.7)
      stop
      end
```

APPENDIX 2

THE BISECTION METHOD

The bisection method, also known as Bolzano method or method of halving the interval, is one of the methods used for solving non-linear equations. It is based on the following theorem.

- If f(x) is continuous for x between a and b, and if f(a) and f(b) have opposite signs, then there exists at least one real root of f(x) = o between a and b.

Suppose that a continuous function f(x) is positive at x=a and negative at x=b, so that there is at least one root between a and b (a and b are found by curve sketching). If we calculate the function at the point of bisection $x = \frac{a+b}{2}$ there are three possibilities

- $f\left(\frac{a+b}{2}\right) = o$ the root is $\frac{a+b}{2}$
- $f\left(\frac{a+b}{2}\right) < o$ the root lies between a and $\frac{a+b}{2}$
- $f\left(\frac{a+b}{2}\right) > o$ the root lies between $\frac{a+b}{2}$ and b

We can see that for any of the two last cases there is a new interval for which the process can be repeated to obtain a smaller and smaller interval within which a root must lie.

The equation obtained in Chapter 3 is: $x - \frac{1}{4}\,Ln(2x) - \frac{1}{2} = o$

We consider the function $f(x) = x - \frac{1}{4}\,\mathrm{Ln}\,(2x) - \frac{1}{2}$. A plot of f(x) (see Fig. a2.1) shows that there are two roots. A direct one which has the value x = 0.5 (this solution is not the wanted one in Chapter 3, because it corresponds to a length which is equal to zero). The other solution lies between a = 0.01 and b = 0.25 where the function changes sign.

One may tabulate as follows

a	0.01	0.01	0.07	0.1	0.1
b	0.25	0.13	0.13	0.13	0.115
$\frac{a+b}{2}$	0.13	0.07	0.1	0.115	0.1075
f(x)	-0.03323	0.06100	0.00236	-0.01758	-0.00822

0.1	0.1	0.1	0.1009	0.1013
0.1075	0.10375	0.1018	0.1018	0.1018
0.10375	0.1018	0.1009	0.1013	0.10155
- 0.993094	-0.0004846	0.00102	0.00043	0.0000064

The flow chart given in Fig. a2.2 may also be used in programming.

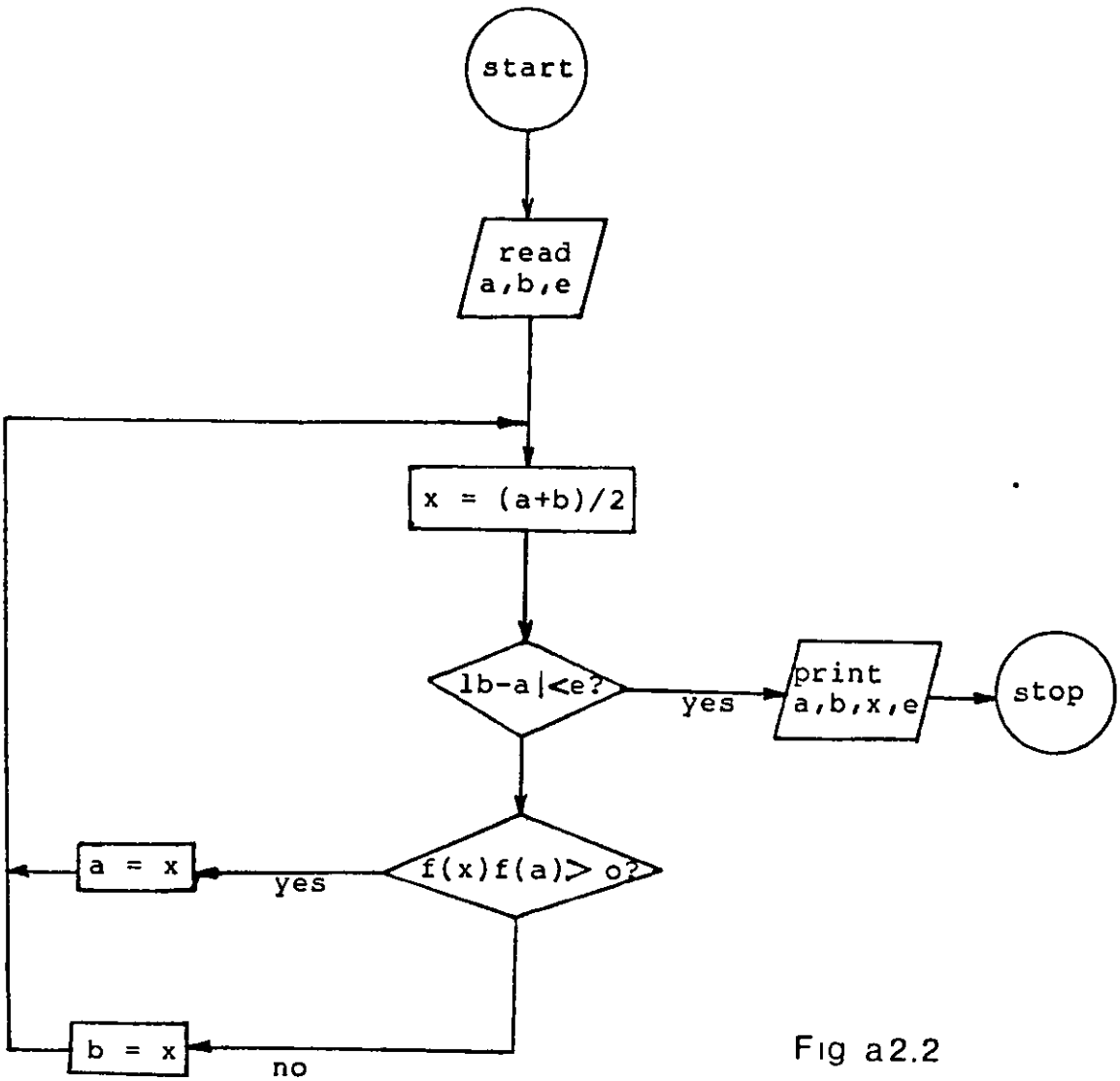

Fig a2.2

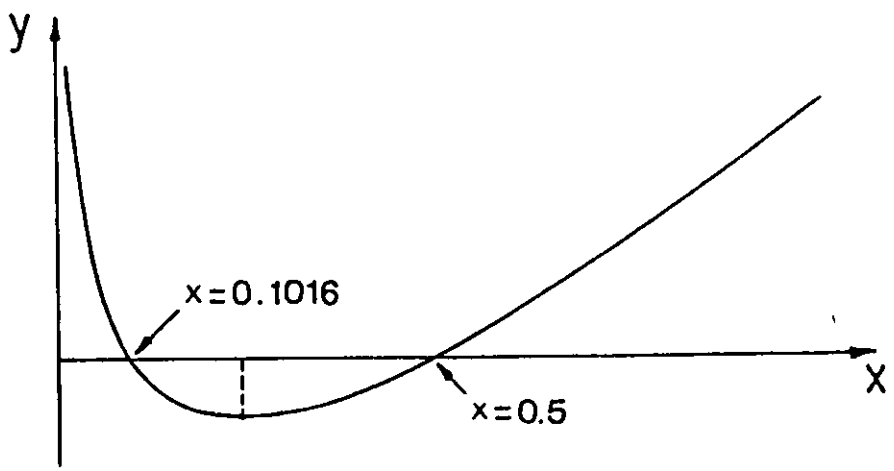

Fig a2.1 Graph of the function $y = x - \frac{1}{4}\ln(2x) - \frac{1}{2}$

APPENDIX 3

ELLIPTICAL APPROXIMATION FOR THE LENGTH OF WIRE OF A D-SHAPE TOROIDAL CAGE

In order to calculate the d.c. resistance of a D-shape toroidal cage, it is necessary to know the length of wire used to construct it. However there is no simple formula available to help compute it. To deal with this problem, a geometrical approximation is used to express the mean turn perimeter in function of the inner perimeter in each sub-coil.

As shown in Fig. a3.1, the dimensionless curve z(r/b) which defines the optimum D-shape may be divided into three parts; one straight leg of length E and two curved parts of lengths P_1 and P_2. The total perimeter is thus given by

$$P = E + P_1 + P_2 \qquad (a3.1)$$

The two curved parts have elliptical appearances, and it is possible to express them, as dimensioned in Fig. a3.1, by the relations

$$P_1 = C_1 (X_1 + Y_1) \qquad (a3.2)$$

where

$$X_1 = \sqrt{\alpha} - 1, \quad Y_1 = z_m - E \quad \text{and} \quad C_1 = \text{cste} \qquad (a3.3)$$

and

$$P_2 = C_2 \, (X_2 + Y_2) \qquad \text{(a3.4)}$$

where

$$X_2 = \alpha - \sqrt{\alpha} \;, \quad Y_2 = z_m \quad \text{and} \quad C_2 = \text{cste} \qquad \text{(a3.5)}$$

Indeed, as seen in Table a3.1, C_1 and C_2 have almost constant values for a range of values of α.

For a n layers elliptical bunch having an equilateral triangular envelope section and with the inner perimeter defined, as dimensioned in Fig. a3.2, by

$$P = C \, (X + Y) \qquad \text{(a3.6)}$$

the length of each layer is

$$\begin{aligned}
&\text{layer 1 :} && l_1 = nC \, (X+Y) \\
&\text{layer 2 :} && l_2 = (n-1) \, C \, (X+Y+2h) \\
&\text{------} && \text{----------} \\
&\text{layer i :} && l_i = (n-i+1) \, C \, [X+Y+2(i-1)h] \qquad \text{(a3.7)} \\
&\text{--------} && \text{----------} \\
&\text{layer n :} && l_n = C \, [X+Y+2(n-1)h]
\end{aligned}$$

The mean turn length of the bunch is then

$$l_{av} = \frac{l_1 + l_2 + \ldots + l_n}{n + (n-1) + \ldots + 1} \qquad \text{(a3.8)}$$

$$= C \, \frac{\sum_{i=1}^{n} (n-i+1)[X+Y+2(i-1)h]}{l} \qquad \text{(a3.9)}$$

$$= C \left[(X+Y)n \frac{\sum 1}{\sum i} - (X+Y) \frac{\sum i}{\sum i} + (X+Y) \frac{\sum 1}{\sum 1} + 2nH \frac{\sum i}{\sum i} \right.$$

$$\left. -2h \frac{\sum i^2}{\sum i} + 2h \frac{\sum i}{\sum 1} - 2nh \frac{\sum 1}{\sum i} + 2h \frac{\sum i}{\sum i} - 2h \frac{\sum 1}{\sum i} \right] \quad \text{(a3.10)}$$

with

$$\sum_{i=1}^{n} 1 = n \ , \ \sum_{i=1}^{n} i = \frac{n(n+1)}{2} \text{ and } \sum_{i=1}^{n} i^2 = \frac{n(n+1)(2n+1)}{6} \quad \text{(a3.11)}$$

it becomes

$$l_{av} = C \left[(X+Y) + \frac{2}{3} (n-1)h \right] \quad \text{(a3.12)}$$

or, using equation (a3.6)

$$l_{av} = P \left[1 + \frac{2(n-1)h}{3(X+Y)} \right] \quad \text{(a3.13)}$$

The dimensionless diameter of wire and the inner radius of the cage are given by

$$\frac{d}{b} = \frac{2h}{\sqrt{3}} \quad \text{(a3.14)}$$

and

$$b = nd \quad \text{(a3.15)}$$

Introducing these equations into equation (a3.13) yields

$$l_{av} = P \left[1 + (1 - \frac{1}{n}) \frac{1}{3(X+Y)} \right] \quad \text{(a3.16)}$$

Applying this result for the D-shape we obtain

$$P_{av} = E + P_1 \left[1 + (1 - \frac{1}{n}) \frac{1}{3(X_1+Y_1)} \right] + P_2 \left[1 + (1 - \frac{1}{n}) \frac{1}{3(X_2+Y_2)} \right] \quad \text{(a3.17)}$$

And the average turn length in each subcoil follows, using equations (a3.3) and (a3.5)

$$\overline{I} = 2b\ P_{av} \tag{a3.18}$$

$$= 2b(E+P_1A+P_2B) \tag{a3.19}$$

with

$$A = 1 + (1 - \frac{1}{n}) \frac{1}{\sqrt{3}(\sqrt{\alpha} - 1 + Z_m - E)} \tag{a3.20}$$

and

$$B = 1 + (1 - \frac{1}{n}) \frac{1}{\sqrt{3}(\alpha - \sqrt{\alpha} + Z_m)} \tag{a3.21}$$

The quantities E, P_1, P_2 and Z_m depend on α and are obtained with the computer program in Appendix 1.

α	3	4	5	6	7	8	9	10
E	0.8469	1.5937	2.4527	3.3949	4.4024	5.4633	6.5692	7.7139
z_m	1.4625	2.4000	3.4169	4.4950	5.6226	6.7916	7.9962	9.2318
P_1	1.0622	1.4262	1.7396	2.0183	2.2714	2.5041	2.7213	2.9244
P_2	2.1366	3.4434	4.8377	6.2978	7.8103	9.3667	10.9595	12.5850
X_1	0.7321	1.0000	1.2361	1.4495	1.6457	1.8284	2.0000	2.1623
Y_1	0.6156	0.8064	0.9642	1.1001	1.2202	1.3283	1.4269	1.5179
X_1+Y_1	1.3477	1.8064	2.2003	2.5496	2.8659	3.1567	3.4269	3.6803
X_2	1.2680	2.0000	2.7639	3.5505	4.3543	5.1716	6.0000	6.8377
Y_2	1.4625	2.4000	3.4170	4.4950	5.6226	6.7916	7.9962	9.2318
X_2+Y_2	2.7305	4.4000	6.1809	8.0455	9.9769	11.9632	13.9962	16.0695
c_1	0.7882	0.7895	0.7906	0.7916	0.7926	0.7933	0.7941	0.7946
c_2	0.7825	0.7826	0.7827	0.7828	0.7828	0.7830	0.7830	0.7832

Table a3.1

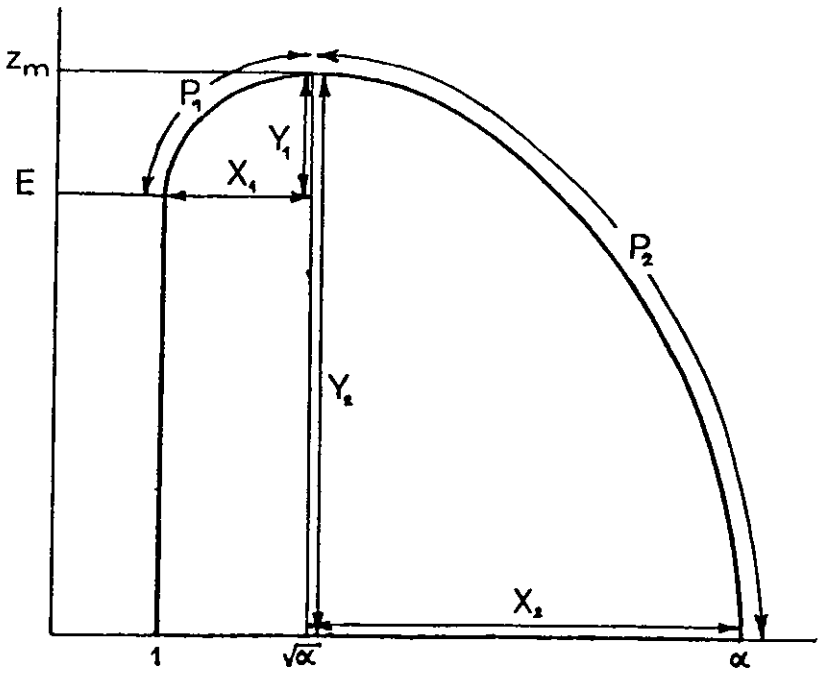

Fig. a3.1

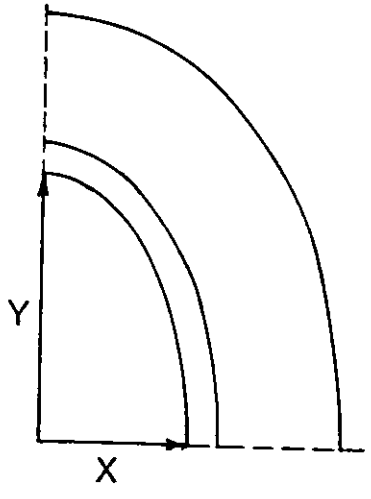

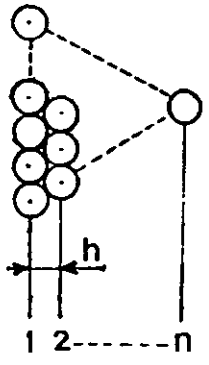

Fig. a3.2

APPENDIX 4

Murgatroyd, P.N., Belahrache, D.: 'Economic designs for single-layer toroidal inductors'. IEE Proceedings, Vol.132, Pt.B, No.6, Nov.1985.

Economic designs for single-layer toroidal inductors

P.N. Murgatroyd, B.Sc., Ph.D., F.Inst.P., C.Eng., F.I.E.E., and D. Belahrache, Dipl.E.S.

Indexing terms Components Industrial applications of power Power electronics

Abstract Maxwell's problem of winding the greatest possible inductance with a given length of wire is examined for single-layer toroids Optimum designs are obtained when the turns are square or circular or the Shafranov D-shape In each case the optimum number of turns is proportional to the square root of the wire length, and the best obtainable inductance increases approximately as the three-halves power of the wire length A simple graphical procedure achieves the most economical design for a required inductance and current rating

List of symbols

L_c = inductance of circle-section toroid
L_s = inductance of square-section toroid
L_D = inductance of D-shape-section toroid
L_0 = $\mu_0 d/2\pi$ = dimensionless inductance unit
μ_0 = permittivity of free space
= $4\pi \times 10^{-7}$ H m^{-1}
d = wire diameter
w = wire total length
k = w/d = dimensionless wire length
N = number of turns
T = major radius of circle-section toroid
R = minor radius of circle-section toroid
A = side of square section
S = inner contact radius for square-section toroid
x = optimising variable
B = inner contact radius for D-section toroid
α = ratio of outer/inner radii, D-section
$z(r)$ = shape function
$S(\alpha)$ = inductance function for D-section
$P(\alpha)$ = perimeter function for D-section

1 Introduction

Air-cored toroidal inductors are used in power electronic circuits because they are relatively easy to make, they do not saturate, and they do not produce troublesome external magnetic fields An interesting design problem for single-layer toroids may be posed as follows 'For a given length of wire, how many turns will provide the greatest self inductance?' A similar problem was posed in the last century by Maxwell, concerning the best way to wind a given length of wire into a solenoid, and the solution is commonly known nowadays as a Brooks coil [1] If the corresponding problem for toroids has been solved, the solution is not at all widely known

The essential features of the problem are shown in Fig 1 Let a given length of wire be wound into a single-layer toroid of a given shape If the number of turns N is large, as in Fig 1*b*, the inductance benefits by the usual dependence on N^2, but the small area of each turn cancels this out if N is large enough, so the inductance is low If the number of turns N is small, the inner toroid radius is small and the turn area is large, both effects benefit the inductance, but the advantage of N^2 is lost It seems intuitively that there must be some compromise, and it will be shown that, for a given shape, there is a value of N that gives a maximum inductance

Paper 4150B (P2, P6 S8) received 30th April 1985

The authors are with the Department of Electronic & Electrical Engineering, Loughborough University Leicestershire LE11 3TU, United Kingdom

A second, and related, problem is the best turn shape This is approached, first, by considering squares and circles, because the inductance formulas are relatively

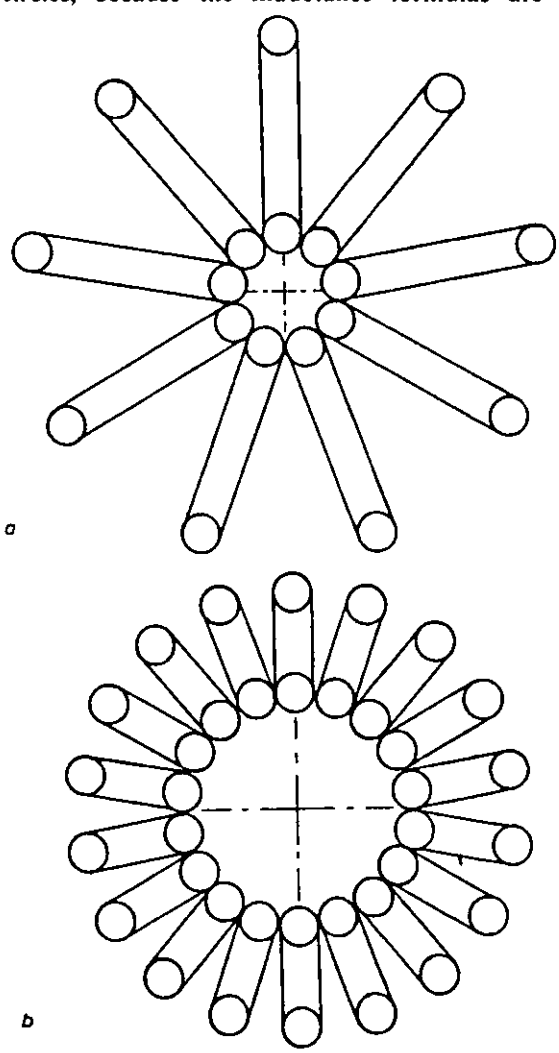

Fig 1 *Plan section of two single-layer toroid inductors using the same wire length in different ways*

simple, and neither shape presents special difficulty of calculation or manufacture As the best shape of all possible thin toroid shapes is known [2, 3], this has also been studied, to give a toroid design which is optimised for both shape and number of turns

2 Circular cross-section

The inductance of a circular-section toroid, as dimensioned in Fig 2, is given by

$$L_c = \mu_0 N^2\{T - \sqrt{(T^2 - R^2)}\} \quad (1)$$

The formula depends on simplifying assumptions which include

(i) the wire thickness is negligible compared with the overall dimensions

(ii) the number of wires is sufficiently large that the field inside the toroid is smooth and the field outside is negligible

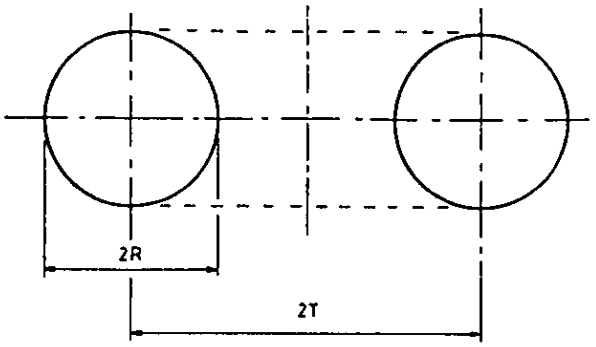

Fig 2 *Ideal single-layer toroidal winding with circular cross-section*

Let the given piece of wire have length w and diameter d Then the minor radius of the toroid is

$$R = \frac{w}{2\pi N} \tag{2}$$

The inner radius of the winding section, $T - R$, is determined by the condition that the N wires just touch around the circumference of the circle as shown in Fig 1

$$\frac{d}{2(T-R)} = \sin\left(\frac{\pi}{N}\right) \tag{3}$$

The inductance is now given by

$$L_c = \mu_0 N^2 \left\{ \frac{d}{2\sin\left(\frac{\pi}{N}\right)} + \frac{w}{2\pi N} - \sqrt{\frac{d}{2\sin\left(\frac{\pi}{N}\right)}\left(\frac{d}{2\sin\left(\frac{\pi}{N}\right)} + \frac{w}{\pi N}\right)} \right\} + \frac{\mu_0 w}{8\pi} \tag{4}$$

where the last term is the 'internal' inductance of the wire It is convenient to express the inductance in terms of a scale inductance

$$L_0 = \frac{\mu_0 d}{2\pi} \tag{5}$$

and to express the wire length as a ratio to the wire diameter, so

$$k = \frac{w}{d} \tag{6}$$

With these substitutions

$$\frac{L_c}{L_0} = N^2 \left\{ \frac{\pi}{\sin\left(\frac{\pi}{N}\right)} + \frac{k}{N} - \sqrt{\frac{\pi^2}{\sin^2\left(\frac{\pi}{N}\right)} + \frac{\pi}{\sin\left(\frac{\pi}{N}\right)}\frac{2k}{N}} \right\} + \frac{k}{4} \tag{7}$$

In Fig 3 the inductance function L/L_0 is plotted against the number of turns N, for a range of values of the dimensionless wire length k The inductance is seen to have a soft optimum The optimum number of turns may be found in principle, by differentiating the function in eqn 7, but this is awkward and no analytical solution has been found The

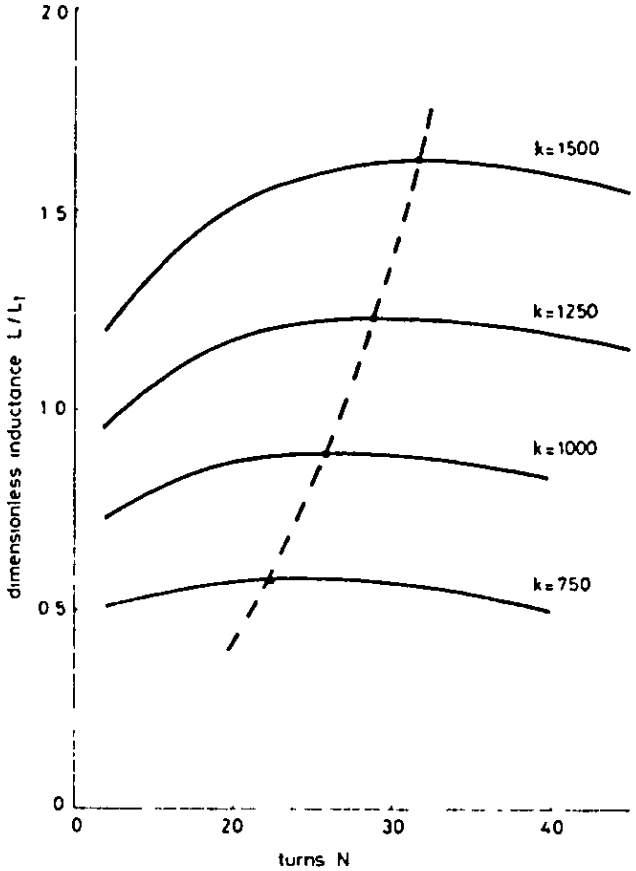

Fig 3 *Dependence of toroid inductance on number of circular turns wire length fixed*

peaks can, however, be found to any required accuracy by tabulation It turns out that, for a given wire length $w = kd$, the best number of turns is closely proportional to $N^{1/2}$ and the best available inductance is closely proportional to $N^{3/2}$ These results are explained by the following approximate analysis, when N is so large that sin (π/N) may be replaced by π/N and

$$\frac{L_c}{L_0} \to N^2 \left\{ N + \frac{k}{N} - \sqrt{(N^2 + 2k)} \right\} + \frac{k}{4} \tag{8}$$

The value of N to maximise this function, obtained analytically, is $0.8165k^{1/2}$ When put back into eqn 8 this delivers the best possible inductance at $0.2722k^{3/2} + 0.25k$

3 Square cross-section

The inductance of a square-section toroid, as dimensioned in Fig 4, is given by

$$L_c = \frac{\mu_0}{2\pi} N^2 A \ln\left(1 + \frac{A}{S}\right) \tag{9}$$

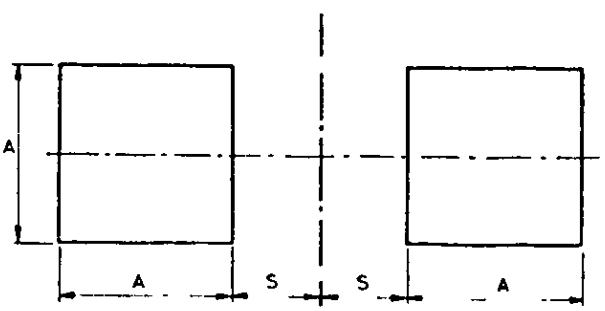

Fig 4 *Ideal single-layer toroidal winding with square cross-section*

The side of the square is

$$A = \frac{w}{4N} \tag{10}$$

and the wire contact condition is

$$\frac{d}{2S} = \sin\left(\frac{\pi}{N}\right) \tag{11}$$

The inductance, including the 'internal' inductance of the wires, is therefore

$$L_s = \frac{\mu_0 N w}{8\pi} \ln\left\{1 + \frac{w}{2Nd}\sin\left(\frac{\pi}{N}\right)\right\} + \frac{\mu_0 w}{8\pi} \tag{12}$$

This formula may be rewritten in terms of the scale inductance L_0 and the dimensionless wire length k introduced previously

$$\frac{L_s}{L_0} = \frac{Nk}{4} \ln\left\{1 + \frac{k}{2N}\sin\left(\frac{\pi}{N}\right)\right\} + \frac{k}{4} \tag{13}$$

The inductance has a soft optimum with general features similar to the circular-section inductor, except that the best square-section inductor has more turns, and gives a best inductance about 8% inferior to the circle If N is large, eqn 13 may be approximated

$$\frac{L_s}{L_0} \rightarrow \frac{Nk}{4} \ln\left(1 + \frac{\pi k}{2N^2}\right) + \frac{k}{4} \tag{14}$$

To make the derivative zero, the equation

$$\ln(2x) - 4\lambda + 2 = 0 \tag{15}$$

where

$$\frac{1}{2x} = 1 + \frac{\pi k}{2N^2} \tag{16}$$

has to be solved The solution, $\lambda = 0.1016$, is obtained numerically and gives the optimum value of N at $0.6329k^{1/2}$ When this is put back into eqn 14 the best available inductance is given as $0.2522k^{3/2} + 0.25k$

4 Shafranov D-shape section

Although the circle section gives the greatest turn area for a given turn perimeter, it does not give the greatest inductance because the flux density is not uniform in the turn The best possible shape, giving the greatest inductance of any shape having a given perimeter, has been calculated by the variational method [2, 3] and it resembles the letter D with the straight part on the inward side, nearest the toroid principal axis The shape is specified by a single number α which is the ratio of maximum and minimum distances from the toroid principal axis, as shown in Fig 5 Unfortunately, the shape $z(r)$, height as a function of radius, does not have a simple analytical form The inductance of a single-layer toroid of fine wires is given by

$$L_D = \frac{\mu_0}{2\pi} N^2 B S(\alpha) \tag{17}$$

where B is the inner radius measured from the toroid principal axis and $S(\alpha)$ is a dimensionless function that must be obtained numerically [3] for each value of shape parameter α The turn perimeter is $BP(\alpha)$, where $P(\alpha)$ is the dimensionless perimeter which is also obtained numerically; so, for N turns from a fixed length w,

$$BP(\alpha) = \frac{w}{N} \tag{18}$$

The wire contact condition is approximately

$$\frac{d}{2B} = \frac{\pi}{N} \tag{19}$$

for large N, as assumed in the previous cases From the last two equations B can be eliminated to give the number of turns

$$N = \left(\frac{2\pi k}{P(\alpha)}\right)^{1/2} \tag{20}$$

The full inductance is now given by

$$L_D = \frac{\mu_0}{2\pi} N w \frac{S(\alpha)}{P(\alpha)} + \frac{\mu_0 w}{8\pi} \tag{21}$$

$$\text{So} \quad \frac{L_D}{L_s} = (2\pi)^{1/2} \frac{S(\alpha)}{P(\alpha)^{3/2}} k^{3/2} + \frac{k}{4} \tag{22}$$

Thus it has been shown that the dependence on the dimensionless wire length k is just the same in this case as for the circle and square, but the optimum value of the radius ratio α has yet to be found From eqn 22, the required value is that which maximises $S(\alpha)P(\alpha)^{-3/2}$, and this quantity is plotted in Fig 6 using values obtained numerically

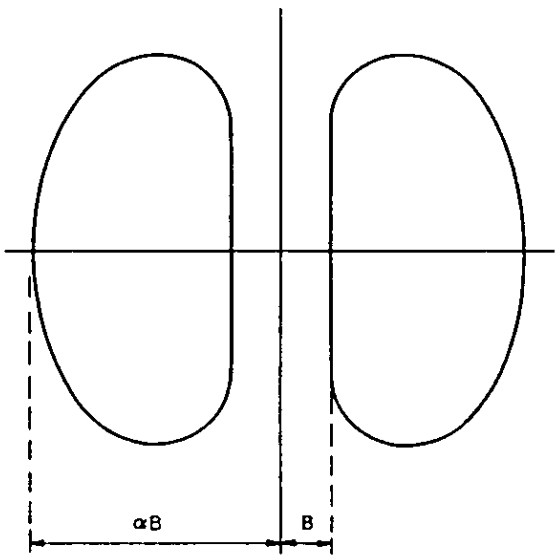

Fig 5 *Geometry of the ideal (Shafranov) toroid cross-section*

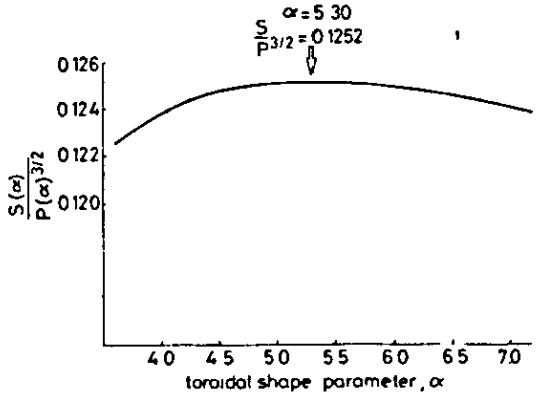

Fig 6 *Graph to locate the optimum value of shape parameter*

by the methods described previously [3] The peak occurs at $\alpha = 5.30$, where $S(\alpha)P(\alpha)^{-3/2} = 0.1252$ and $P(\alpha) = 19.69$ With these values the optimum number of turns is found to be $0.5649k^{1/2}$ and the best available inductance is $0.3139k^{3/2} + 0.25k$ This inductance is (comparing just the first terms for large k) about 15% better than the best circle, which was itself about 8% better than the best

square In Fig 7, the Shafranov shape with $\alpha = 5.3$ is plotted on a square grid, to facilitate copying

The complete results for the best designs of each turn

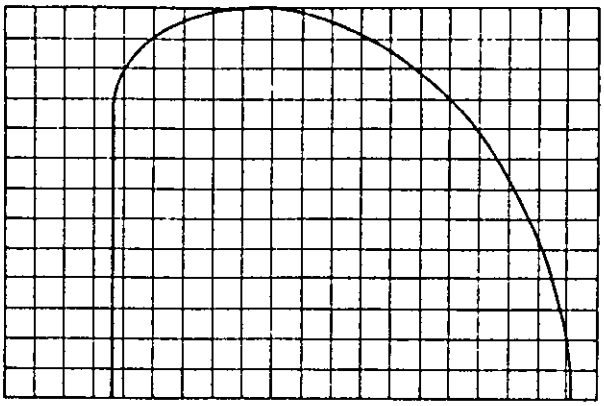

Fig 7 *Optimum toroid cross-section with* $\alpha = 5.3$

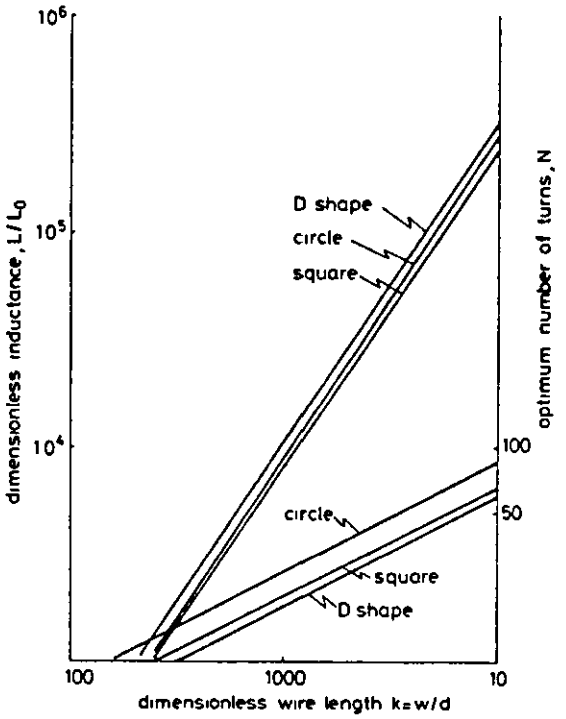

Fig 8 *Design graphs for most economic single-layer toroids*

shape are summarised in Fig 8 The horizontal scale is the dimensionless wire length k. The right vertical scale is the optimum number of turns N, which is given by three parallel lines with slope 0.5 The left vertical scale is the best available inductance L/L_0, given by three nearly parallel graphs with slope approximately 1.5

5 Practical example

A toroidal inductor is required for a railway traction chopper circuit, with the following major properties $L = 12.7$ μH (±10%), current rating 390 A RMS, circle section The design procedure is as follows

(*a*) Choose conductor diameter Assuming solid round conductors with current density $J = 4$ A mm^{-2} the calculated diameter is impractically large at 11.1 mm For flexibility, and current sharing against eddy-current effects, a many-stranded braid is used with nominal diameter 20.4 mm

(*b*) Calculate the base inductance L_0

$$L_0 = \frac{\mu_0 d}{2\pi} = 2 \times 10^{-7} \times 20.4 \times 10^{-3} = 40.8 \times 10^{-10} \text{ H}$$

(*c*) Find the dimensionless inductance

$$\frac{L}{L_0} = \frac{12.7 \times 10^{-6}}{40.8 \times 10^{-10}} = 3113$$

(*d*) Use the graph (Fig 8) to find the full length of conductor required

$$k = \frac{w}{d} = 495, \quad w = 10.1 \text{ m}$$

(*e*) Use the graph (Fig 8) to find the number of turns, and hence the dimensions of the toroid

$N = 18$ (nearest integer)

$$R = \frac{w}{2\pi N} = 89.3 \text{ mm}$$

$$T = R + \frac{d}{2 \sin(\pi/N)} = 148.0 \text{ mm}$$

(*f*) Check the calculation using

$$L = \mu_0 N^2 \{T - \sqrt{(T^2 - R^2)}\} + \frac{w}{8\pi} = 12.71 \ \mu\text{H}$$

and note that in this example the 'internal' inductance provides just over 4% of the total

The economic value of using the best value of N in this particular example is well worthwhile An earlier design of coil, without benefit of these calculations, needed about two metres more braid, and the potential saving on production of over a hundred coils is of the order of thousands of pounds This may be increased considerably by using a Shafranov D-shape toroid

In practice, of course, it is not always possible to use the most economic design because it may not fit into the space allowed in the overall electronic system Designing a less economic inductor is then a matter of trial and error, trading turns against size Even so, it is pleasing to note that the graphical method given here makes it easier to get the most economic design than it is to get any inferior design by trial and error

6 Acknowledgment

The work of D Belahrache is made possible by a scholarship from the Democratic and Popular Republic of Algeria

7 References

1 BROOKS, B 'Design of standards of inductance and the proposed use of model reactors in the design of air-core and iron-core reactors', Research paper 342, *J Res NBS* 1931, **7**, pp 289–328

2 SHAFRANOV, V D 'Optimum shape of a toroidal solenoid', *Sov Phys-Tech Phys*, 1973, **17**, (9), pp 1433–1437

3 MURGATROYD, P N 'Some optimum shapes for toroidal inductors', *IEE Proc B, Electr Power Appl* 1982, **129**, pp 168–176